Journal of Coastal Research	9	2	539–576	Fort Lauderdale, Florida	Spring 1993

Alluvial Stiff Muds (Late Pleistocene) Underlying the Lower Nile Delta Plain, Egypt: Petrology, Stratigraphy and Origin

Zhongyuan Chen and Daniel Jean Stanley

Mediterranean Basin Program
E-207 NMNH, Smithsonian Institution
Washington, D.C. 20560 U.S.A.

ABSTRACT

CHEN, Z. and STANLEY, D.J., 1993. Alluvial stiff muds (late Pleistocene) underlying the Nile delta plain, Egypt: Petrology, stratigraphy and origin. *Journal of Coastal Research*, 9(2), 539–576. Fort Lauderdale (Florida), ISSN 0749-0208.

Stiff muds of late Pleistocene age, interbedded with alluvial sands, are buried beneath Holocene deposits of the Nile delta in Egypt. The origin of the muds are interpreted on the basis of the petrology, stratigraphy and distribution of radiocarbon-dated sections recovered in cores across the northern delta. Four distinct stiff mud sequences, or subfacies, are defined on the basis of lithology, sand-sized composition and clay mineralogy. These sequences include (I) calcareous nodule-, (II) gypsum nodule-, (III) shell- and (IV) plant debris-bearing stiff muds. They accumulated: I, in seasonally flooded inland sebkhas proximal to Nile channels, which were then covered with wind-blow sand; II, in somewhat more central sectors of such playas, more distal to flood channels; III, in more permanent salt lakes; and IV, in freshwater to low salinity marshes adjoining seasonally flooded playas. Sequence I, the dominant lithofacies, is concentrated in 14 geographically distinct lithosomes. Sequence II occurs at or near the center of these lithosomes, while III and IV are more localized. Spatial and temporal distribution of muds suggest a predominance of incised channels in the north-central Nile alluvial plain, and more laterally migrating channels to the northeast and northwest.

Most stiff mud layers, deposited earlier than 34,000 and at ~28,000–22,000 and ~16,000–>10,000 years BP, are correlated with several late Pleistocene aggradational phases of the Nile in upper Egypt. The more time-restricted gypsum nodule-bearing sequence II accumulated primarily during a period of increased aridity. Lower alluvial plain muds are also correlated with deposits of equivalent age offshore, on the Nile Cone. Paleogeographic reconstructions indicate that River Nile sediments bypassed the northwestern delta plain and were deposited on the Cone. Nile stiff mud facies, primarily sequences I and III, are compared with those of equivalent age in Yangtze and Mississippi delta cores. Gypsum-rich subfacies (sequence II) are regionally more restricted to warm, arid regions such as the Nile. We postulate that stiff muds underlie Holocene sections in all major delta plains, having accumulated at times of eustatic lowstands. Their petrology and distribution patterns are best explained in terms of depositional setting, fluvial sediment load and flood patterns, and especially, climate. The nature and configuration of stiff muds has practical applications for civil engineering and construction purposes in deltaic settings, and also for hydrocarbon exploration.

ADDITIONAL INDEX WORDS: *Alluvial plain, alluvial sands, coastal sediments, delta deposits, deltaic formation, Nile shelf, stratigraphic sequence.*

INTRODUCTION

The modern Nile delta of Egypt is almost completely blanketed by Holocene sediments, commonly termed Nile silts, which range in thickness from about 5 to 50 meters (SAID, 1981; STANLEY, 1990). The underlying late Quaternary deposits are only locally exposed in small topographic mounds, called geziras or turtlebacks (BUTZER, 1976), and little is known of their petrology, stratigraphic distribution and origin. In a series of early studies, FOURTAU (1899, 1915) described the subsurface interbedded sands and compact muds in cores recovered in the Nile delta. This was updated by ATTIA (1954) who presented an extensive listing of core descriptions and generalized cross-sections. More recent attention was paid to the delta's subsurface geology by BUTZER (1976) and UNDP/UNESCO (1978). All of the above investigations show that interfingering sands and muds underlie Recent deltaic plain deposits, and that muds are much less widely distributed than sands. The sands, mostly iron-stained quartz, have been interpreted in all previous studies as Nile alluvial deposits.

Until recently, little attention was paid to the late Pleistocene subsurface muds. A series of recent analyses (COUTELLIER and STANLEY, 1987; FRIHY and STANLEY, 1988; ARBOUILLE and STANLEY, 1991; CHEN *et al.*, 1992; STANLEY *et al.*, 1992; WARNE and STANLEY, 1993) have compiled

92097 received and accepted in revision 5 October 1992.

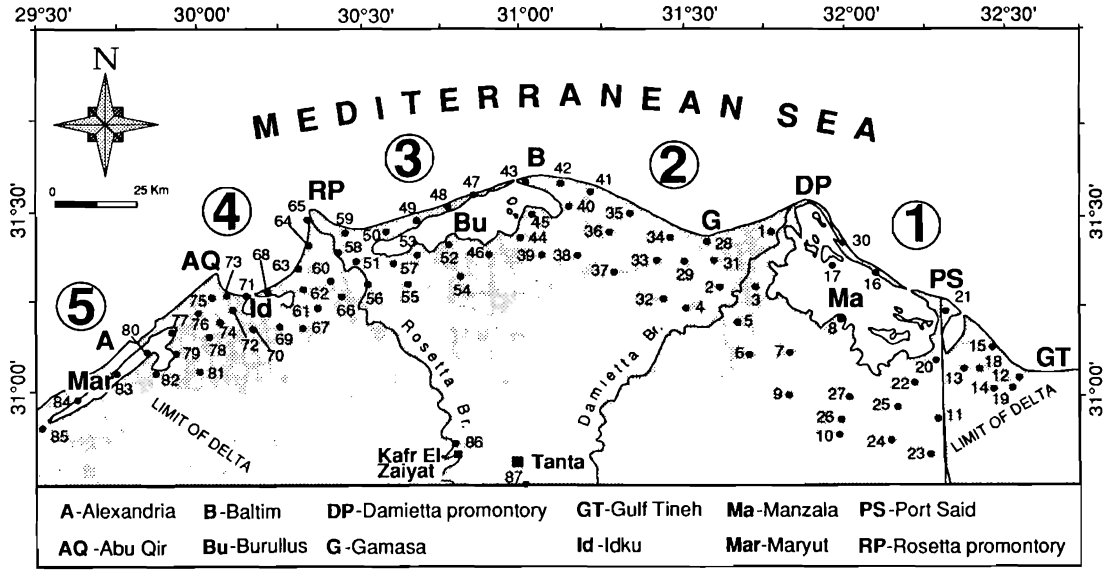

Figure 1. Map of the northern Nile delta, Egypt, showing positions of the 87 Smithsonian borings examined and localities cited in this study. Large circled numbers refer to detailed regional investigations, from east to west: (1) COUTELLIER and STANLEY, 1987; (2) STANLEY *et al.*, 1992; (3) ARBOUILLE and STANLEY, 1991; (4) CHEN *et al.*, 1992; and (5) WARNE and STANLEY, 1993.

information on this facies during a systematic coring program across the entire northern Nile delta conducted as part of the Smithsonian Institution's Nile Delta Project (Figure 1). These studies have shown that the late Pleistocene muds are markedly different from those in overlying Holocene sections. The Project has provided a large information base with which to determine chronostratigraphic distribution and origin. In contrast with some earlier studies (UNDP/UNESCO, 1978; SESTINI, 1989), we now recognize that this facies accumulated when the lower Nile plain was subaerially exposed and not influenced by the sea. However, in order to further refine interpretations of the pre-Holocene evolution of the Nile delta, a more comprehensive investigation of late Quaternary facies in the lower plain is warranted.

In the Nile delta study area, fine-grained deposits of late Pleistocene age have previously been termed compact clay (FOURTAU, 1899; ATTIA, 1954) and stiff clay (COUTELLIER and STANLEY, 1987; WUNDERLICH and ANDRES, 1991). Herein, we refer to these as stiff mud. The present investigation merges the existing Nile delta core petrology database (MEDIBA, 1992) with additionally acquired lithological, mineralogical and stratigraphic information on these stiff muds. Focus is paid to their petrology, chronostratigraphy, and regional distributions to refine interpretations of the evolution and paleogeography of the Nile delta during the late Pleistocene.

In this respect, it is necessary to distinguish and describe the various stiff mud subfacies, herein termed sequences. A primary aim is to identify and interpret the various hard silt and clay admixtures from core sections, and also from hand specimens alone. As part of the investigation, a specific examination is made of Holocene compact alluvial facies on the Nile delta plain which can provide some information on the formation of late Pleistocene stiff muds. It is anticipated that such analyses can shed light on major controlling factors, primarily climate and depositional environment.

Of special consideration is the paleogeographic configuration of the lower delta plain, and the effects of climatic cycles and eustatic oscillations prior to the Holocene. Numerous radiocarbon-dated sections of stiff muds (to >38,000 years BP) enable us to correlate lower delta plain depositional events with those in the Nile valley to the south, and also with offshore Mediteranean sectors to the north. Pleistocene stiff muds are not unique to the Nile. We have examined quite sim-

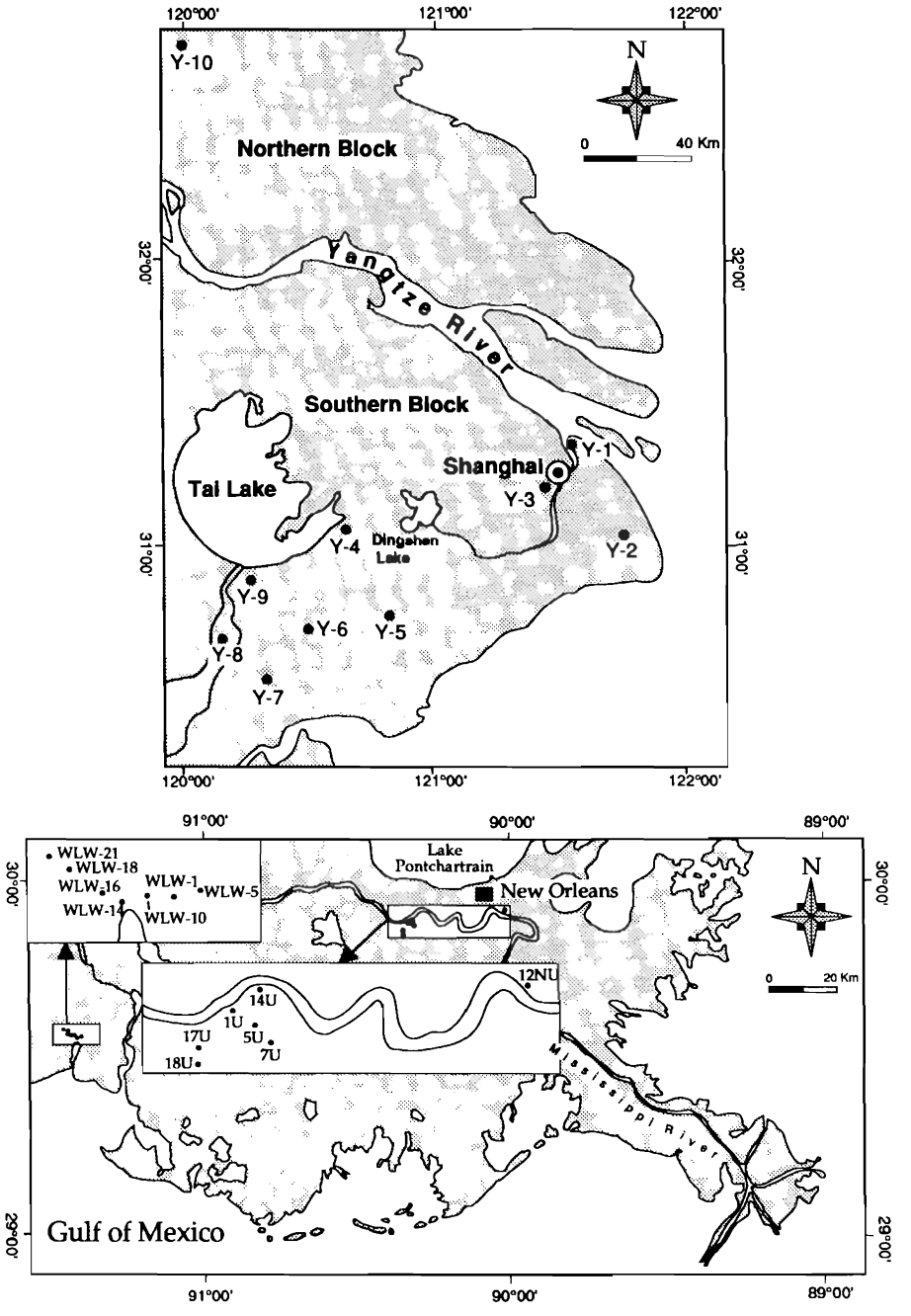

Fig.2

Figure 2. Maps showing positions of cores with stiff mud sections of late Pleistocene age, recovered in the Yangtze delta of eastern China (upper) and Mississippi delta on the U.S. Gulf Coast (lower), examined in this study.

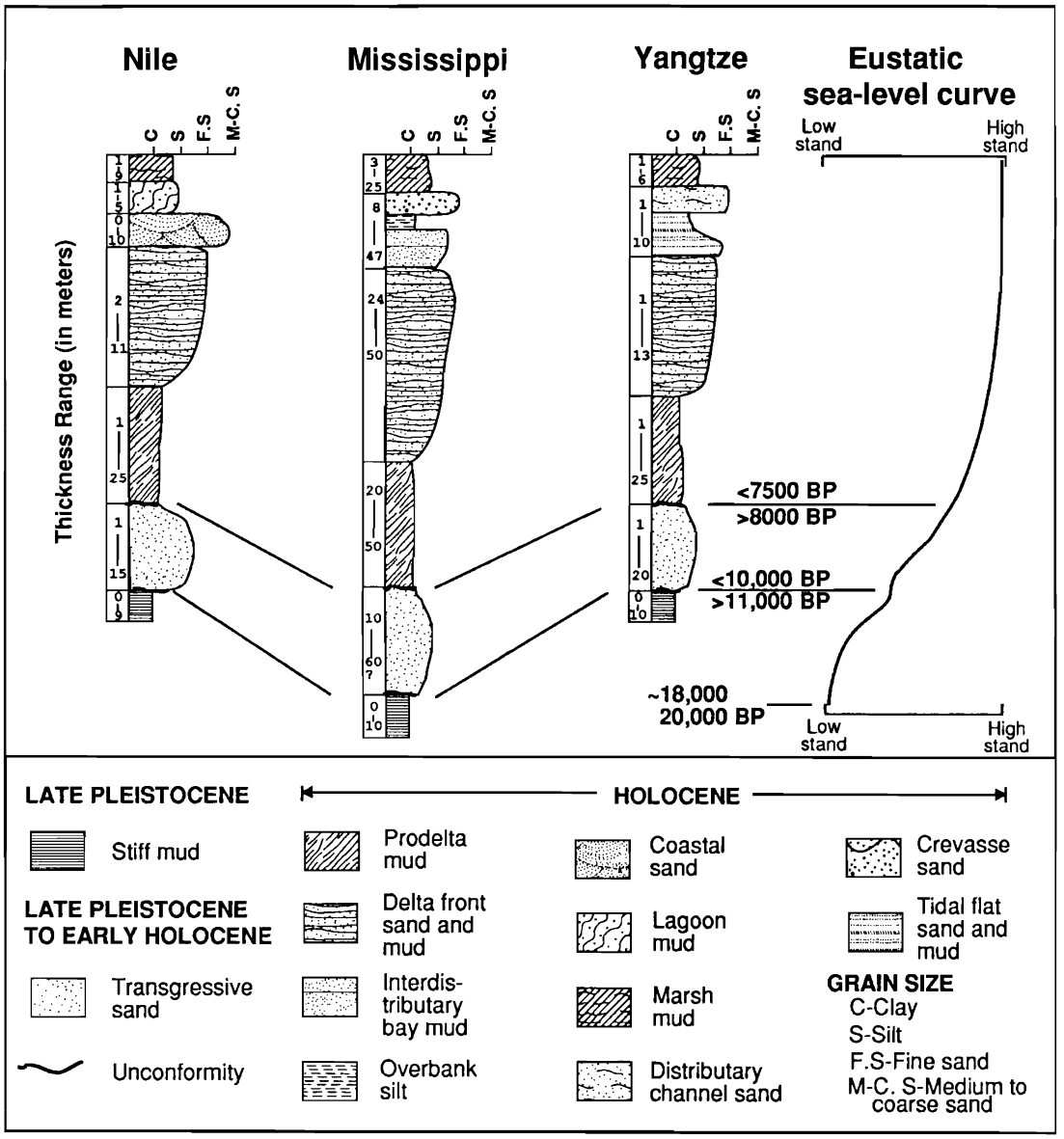

Figure 3. Generalized lithostratigraphic sections from the Nile, Yangtze and Mississippi deltas, showing position of late Pleistocene stiff muds underlying various Holocene delta plain facies. The simplified Mississippi delta section is modified from compilations of SCRUTON (1960) and COLEMAN (1982). Correlations are based on radiometric dates. Sections are related to eustatic sea level changes during the late Quaternary. Generalized sea-level curve, on right, after LIGHTY *et al.* (1982), FAIRBANKS (1989), and others.

ilar examples from the Yangtze off eastern China, the Mississippi in the Gulf Coast (Figures 2, 3), and lithologically similar sections of equivalent age in other deltas described in the literature. These deposits record the periodic subaerial exposure of lower delta plains in different parts of the world as a result of eustatic sea level changes. It would thus be expected that late Quaternary deposits underlying the lower plains of all deltas include subsurface stiff mud layers that interfinger with alluvial sands. Increased knowledge of this cohesive facies has practical applications for

civil engineering design and construction in deltaic settings and for petroleum exploration in deltaic formations.

METHODOLOGY

Eighty-seven continuous sediment borings distributed in the lower plain of the northern Nile delta were examined (Figure 1). Borings are 7.5 cm in diameter, range in length from ~11 to 54 m, and are spaced ~6 to 12 km apart. Most penetrated Holocene to uppermost Pleistocene sequences. Of these, 42 cores recovered 50 layers of Late Pleistocene stiff mud, usually interbedded with medium-grained sands. These layers range in thickness from 0.2 to 10 m, and the total thickness of stiff mud in the 50 layers available for study is about ~103 m. The cores were collected using a trailer-mounted rotary percussion (Acker-2) drilling rig, and were recovered during five Smithsonian expeditions: 1985 (cores S-1 to S-17), 1987 (S-18 to S-30), 1988 (S-31 to S-46), 1989 (S-47 to S-65), and 1990 (S-66 to S-87).

All stiff mud core sections were split and logged on the basis of visual examination and X-radiography. A record was compiled of color, stratal boundaries of physical and/or biogenic origin, mudcracks, caliche structures, calcareous nodules and gypsum crusts, zones of Fe and Mn oxide, fossils, plant debris and root traces.

Petrography of 214 samples collected from all 50 late Pleistocene stiff mud layers were studied in more detail. Samples of stiff mud were collected at each lithological boundary, or at less than 50 cm intervals in thick homogeneous sections. Proportions of clay (<2 μm), silt (2–63 μm), and sand (>63 μm) were determined for each mud sample. Petrographic analysis of the sand-size fraction (*cf.* method of COUTELLIER and STANLEY, 1987) was used to distinguish major compositional components. For each sample, the relative percentages of 15 sand-size components were calculated from point counts of >300 grains (*cf.* method of FRIHY and STANLEY, 1988). These include: 10 mineralogical (light and heavy mineral, mica, glauconite/verdine, pyrite, gypsum, lithic fragment, aggregate, unidentified carbonate particle, Fe/Mn oxide); 4 faunal (unidentified shell fragment, and whole shells of mollusc, foraminifera and ostracod); and 1 floral (diatom, plant fragment and seed). Values for the 15 sand-sized components in representative samples are listed in Table 1.

Most (70–90%) of the sand-sized grains previously defined as terrigenous aggregate particles in calcareous-bearing stiff muds are actually calcareous nodules and calcareous aggregates. Thus, to improve the quality of data in the above 214 samples, a second study was made of the sand fraction of 63 samples. These latter were petrographically examined to better distinguish calcareous nodules (Figure 4A and D) and calcareous aggregates (Figure 4B) from terrigenous aggregates (Figure 4C). Tabulated data for all Nile core samples in the two groups (n = 214, n = 63) are available from the authors.

Analysis of clay minerals (<2 μm) was made of an additional 56 stiff mud samples selected from 42 late Pleistocene layers in 37 borings (Table 2) evenly distributed across the northern Nile delta plain. For comparison, clay mineral analyses were made of 2 samples from Holocene stiff mud layers in 2 borings (S-86 and S-87) in the central Nile delta (Figure 1), and 3 samples from three late Pleistocene Nile valley mud formations (Table 2). Slides were prepared using the pipette method, and analysis of the 61 samples was made using a Philips Norelco diffractometer unit. For verification of results, twelve of the slides were also examined using a Scintag Computer-Automated Powder X-ray diffractometer. Proportions of clay minerals were determined using the peak height method (*cf.* ABU-ZEID and STANLEY, 1990). Composition of three calcareous nodules, two gypsum nodules and three jarosite-rich samples from Nile delta borings were determined by XRD.

Molluscs were identified in one shell-rich stiff mud sample from core S-28 (M.P. BERNASCONI, *written communication*, 1992). A penetrometer was used to measure hardness of all core sections examined; values were obtained at about 0.5 m or less intervals in the field immediately after core recovery, and also after splitting of cores in the laboratory. Most hardness values approximate, or exceed, 3.0.

Radiocarbon dating, using total organic matter and/or minor plant debris/shells, was made of 48 late Pleistocene Nile boring stiff muds. Of these, 46 provided viable dates (Beta Analytic, Inc.; listed in MEDIBA, 1992) and are used to establish a chronostratigraphic framework. Dates of representative samples are shown in Table 1.

For comparative purposes, petrologic studies were made of: 3 samples of late Pleistocene muds collected from the Nile valley (1 from near Beni Suef, 2 from Wadi Kubannia near Aswan); 46 samples from compact Holocene mud sections in two borings (S-86, S-87) in the central Nile Delta

Table 1. *Grain size and composition of the sand-size fraction of representative samples from different stiff mud deposits discussed in this study.*

Facies	Sample number	Grain size			Major components (%)		Accessory components (%)													Age (YBP)
		Sand (%)	Silt (%)	Clay (%)	Light mineral	Heavy mineral	Mica	Glauco./ verdine	Pyrite	Gyp-sum	Lithic frag.	Calc. nodu./ aggregate	Unident. carbon.	Fe/Mn oxide	Shell frag.	Foram	Ostra-cod	Sponge spicule	Plant debris	
Nile delta stiff mud (late Pleistocene, N=214)																				
Sequence I	S-36-12	50.2	35.3	14.5	10.0	1.0						83.0	1.0				1.0		4.0	~26,000
	S-38-18	1.0	33.5	65.5	11.4	0.8	0.8			1.1		78.0	7.9							~22,000
Sequence II	S-14-12	32.3	26.0	41.7	40.9	0.7				47.9		6.4							4.1	~27,000
	S-53-9	1.2	8.0	90.8	75.9	2.6	5.8	1.6	0.3	3.2		0.6	10.0							~28,000
Sequence III	S-47-34	9.5	12.0	78.5	66.1	6.2		0.7			0.7				13.2	9.9	3.3			~27,000
	S-28-24	1.0	45.3	53.7	55.1		6.4				21.3				2.7	8.8	1.3		4.4	~11,000
Sequence IV	S-50-20	0.4	46.9	52.7	8.7	0.3	1.0					2.7						2.6	84.7	~12,000
	S-52-34	11.4	10.1	78.6	63.1	3.8	1.3	1.0	5.3			2.5							23.0	~10,500
Central Nile delta stiff mud (Holocene, N=46)																				
Flood Plain	S-86-35	15.5	77.6	6.9	72.3	1.0	0.7			1.6		23.8							0.7	~3500
	S-87-5	11.5	59.8	28.7	61.2	2.8	0.3			0.6		33.1							1.9	~5000
Nile valley stiff mud (late Pleistocene, N=3)																				
Nile terraces and wadis	Kubbania #1	9.8	80.3	9.9	43.2	0.9	30.0			3.6		22.4								~25,000
	Kubbania #2	74.1	0.8	25.1	92.0	0.3	2.3			1.9	1.9	1.6								~25,300
	Beni Suef	62.9	33.6	3.5	87.9	1.7	4.4			4.7		1.4								>39,000
Yangtze delta stiff mud (late Pleistocene, N=2)																				
Flood Plain	Y-3	3.1	84.3	12.6	31.6	1.3	2.2		0.3			61.3							3.4	~12,000
	Y-10	5.6	25.3	69.1	80.7	1.3	3.9					8.5							5.6	?
Mississippi delta stiff mud (late Pleistocene, N=18)																				
Flood Plain	WLW-18U	3.4	82.3	14.3	68.6		0.7					25.5	1.6	0.3					3.3	~20,000
	WLW-14U	2.2	54.4	43.4	24.2							38.6	31.1	2.6					3.6	~?
Interdis. bay	12NU-20B	65.6	29.1	5.3	90.4	2.2	0.6				1.3	1.9			1.3	1.6			0.6	~8000

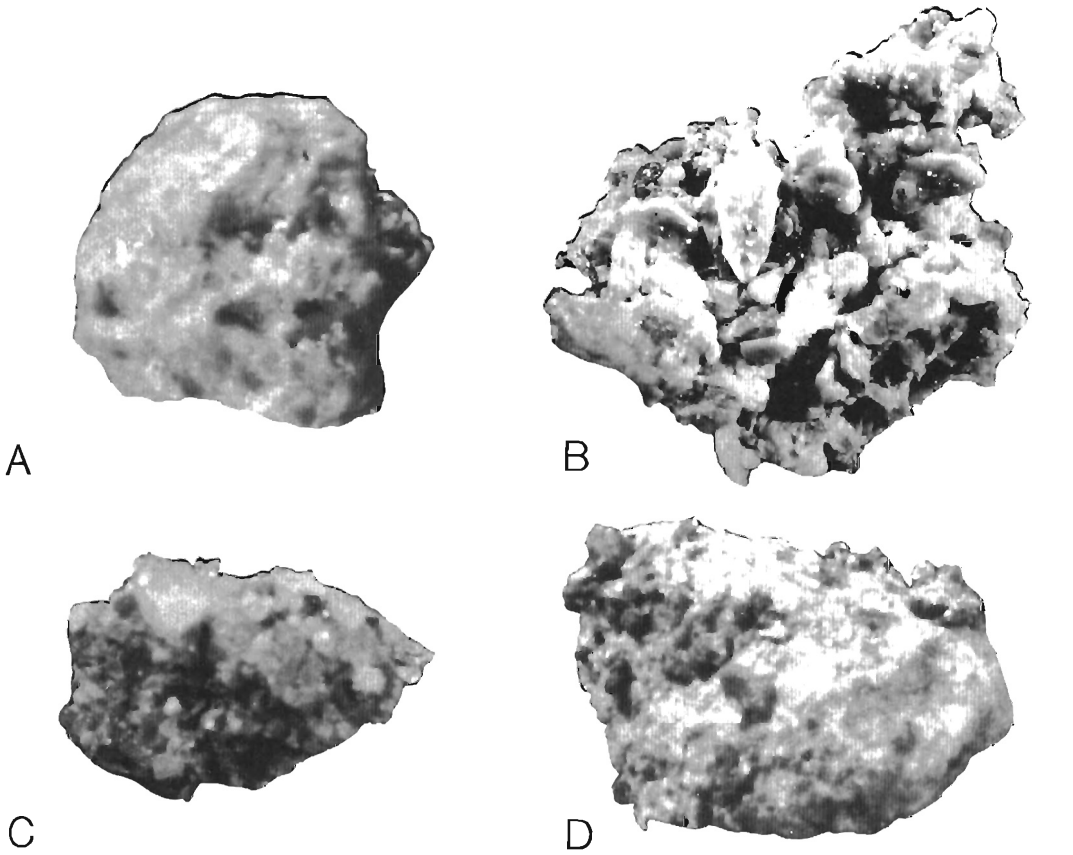

Figure 4. Photomicrographs of representative coarse sand-sized granular particles selected from Nile stiff muds (A–C, late Pleistocene; D, Holocene) A, calcareous nodule (maximum diameter, m.d., = 1.8 mm) of type most commonly found in stiff muds of the lower Nile alluvial plain (core S-53, section VIII, depth ~10.5 m). B, coarse aggregate (m.d. = 2.3 mm) of cemented carbonate sand and silt particles (core S-38, section XVI, depth ~18.5 m). C, aggregate (m.d. = 1.9 mm) of cemented terrigenous silt and sand particles (core S-50, section XXI, depth ~24.3 m). D, calcareous nodule (m.d. = 2.4 mm; core S-87, section V, depth ~4.0 m), similar to A.

(Figure 1); and 2 late Pleistocene stiff mud samples from 2 cores in the Yangtze delta, and 18 samples from 14 cores in the Mississippi delta (Figure 2). These 69 samples were treated in exactly the same manner as the 214 stiff mud samples from the northern Nile delta cores. In addition, petrological data of 8 stiff mud layers from 8 cores in the Yangtze delta (Figure 2) were used in this investigation. Eleven radiocarbon dates (Beta Analytic, Inc.) were obtained for some of these sections (Table 1): 5 for Holocene compact mud samples in the central Nile delta (cores S-86, S-87); 3 for Nile valley samples; 1 for a Yangtze delta core section; and 2 for Mississippi delta core sections. These and previously published dates of sediments in the Yangtze and Mississippi deltas were used to establish chronostratigraphic correlations.

MAJOR LITHOFACIES SEQUENCES

Stiff mud is considered here as one of the major facies of the late Pleistocene age in the Nile delta, as defined by COUTELLIER and STANLEY (1987) and FRIHY and STANLEY (1988). Core sections of stiff mud are rarely uniform, and generally comprise several distinct petrologic intervals. Four distinguishable stiff mud subfacies, or sequences (coded I to IV), are identified on the basis of as-

Table 2. *Proportion of clay minerals (averaged data) from the different stiff mud deposits discussed in this study; ± values represent 1 standard deviation.*

Facies	Age	Number of samples (n)	Smectite (Average %)	Kaolinite (Average %)	Illite (Average %)
Nile delta Sequence I	Late Pleistocene	40	50±10.9	34±7.4	16±7.7
Nile delta Sequence II	Late Pleistocene	10	48±14.6	38±15.6	14±10.3
Nile delta Sequence III	Late Pleistocene	4	44±6.9	35±4.4	21±7.5
Nile delta Sequence IV	Late Pleistocene	2	31±0.1	50±0.1	19±0.1
Nile valley	Late Pleistocene	3	67±14.6	15±3.2	18±14.7
Central Nile delta *	Holocene	2	58±8.2	35±13.4	7±5.2
River Nile channel **	Modern	3	71±5.5	17±3.2	12±2.5
Yangtze delta	Late Pleistocene	2	12±6.6	47±9.9	41±3.3
Mississippi delta	Late Pleistocene	2	41±7.1	29±11.0	30±3.9

* Smithsonian cores S-86, S-87

** Data from ABU-ZEID and STANLEY (1990)

semblages of specific lithologic intervals, termed units (Figure 5). At least nine distinct units (coded A to I, Figure 5) that form sequences are recognized. Units are distinguished by sediment color, general grain size, stratification, structures, and presence of fauna, flora and nodules. Definition of sequence is based largely on vertical succession of units and also on the nature of lithofacies underlying the succession. As in all natural systems, there are variations to the sequences depicted in Figure 5 and described below. Sequence definition is sufficiently flexible to allow all late Pleistocene Nile delta stiff mud sections in cores to be assigned to one of these four major sequences. A description of the four sequences and the 9 units that form them follows. Composition of the sand-size and clay fractions in each of these sequences is discussed in the following section of this article.

Sequence I, Calcareous Nodule-Bearing Stiff Mud

This subfacies is formed by an upward sequence of units A, B, and C, and occurs in 36 cores. Color of sediment is generally yellowish brown. It has a maximum thickness of 3.4 m and usually lies directly above iron-stained, quartz-rich alluvial sand of late Pleistocene age.

Unit A, forming the base of the sequence, is a dark yellowish orange (10YR 6/6) silt and silty clay, ranging in thickness from 0.1 to 0.6 m. Fining-upward texture prevails. Unidirectional bedding (such as climbing ripples; see Figure 6A) is locally present; calcareous nodules occur rarely (formed *in situ*) and are randomly distributed. Large pebbles (with maximum diameter ranging from 6.0 to 9.0 cm) are locally dispersed in some mud sections (STANLEY *et al.*, 1992).

Unit B, above unit A, is a pale yellowish brown (10YR 6/2) mud (Figure 7A) ranging in thickness from 0.1 to 2.2 m. This unit is characterized mainly by both layered and randomly distributed calcareous nodules (Figures 6B and 7A) and vertically-oriented carbonate (caliche) cement structures and mud cracks. Thin sinuous and horizontal silt laminations are locally present (Figure

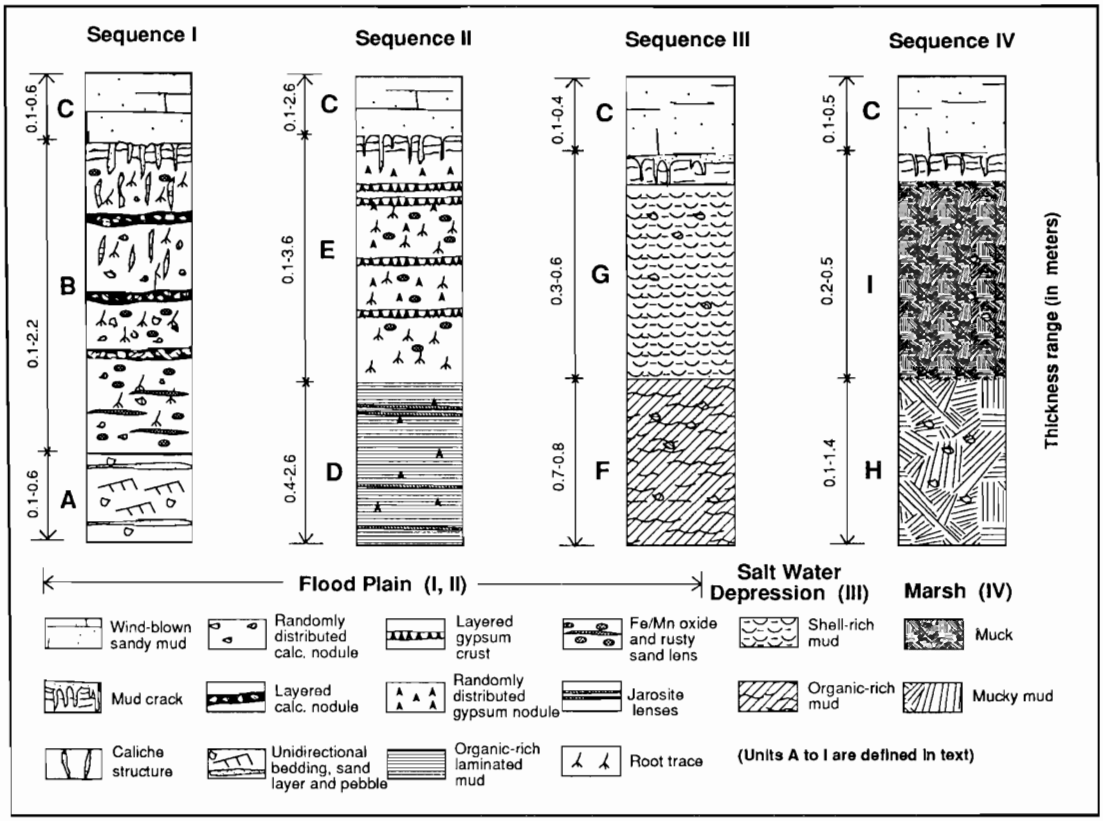

Figure 5. Generalized stiff mud subfacies (sequences I to IV) defined in the Nile delta; sequences are formed by associations of 9 depositional units (A to I, defined in text). Stiff mud sequence I = calcareous nodule-bearing; II = gypsum nodule-bearing; III = shell-bearing; IV = plant debris-bearing. Interpretation in text.

6B and C). There is a generally low content of organic matter. Rusty colored root traces occur in some sections, and oxidized sand lenses and speckled Fe/Mn oxide mud are locally present. Layered nodule horizons, usually 2 to 4 cm in thickness, may occur repeatedly within the unit. Caliche structures, including vertical tubes, are present either above and/or between layered nodule horizons. Mud cracks are best developed at the top of unit B and usually are filled with sand. The lithological contact between units A and B is gradational.

Unit C, which commonly lies above unit B, comprises light brown (5YR 5/6) sandy mud and ranges in thickness from 0.1 to 0.6 m. This sandy mud appears structureless, and is separated by a sharp lithologic contact with underlying unit B. The proportion of sand (largely well-stained quartz grains) mixed with silt and clay usually ranges to 30 to 40 percent.

The association of sedimentary features forming sequence I records various conditions of flood plain deposition which prevailed in the sector underlying the present lower Nile delta plain. The 29 radiocarbon dates available for this sequence indicates that deposition prevailed during two major periods: >38,000–19,000 years BP and ~14,000–11,000 years BP.

Sequence II, Gypsum Nodule-Bearing Stiff Mud

This subfacies comprises units D, E, and C and occurs in 10 cores. This sequence has a maximum thickness of 8.8 m, and basal unit D lies directly above late Pleistocene alluvial to shallow marine

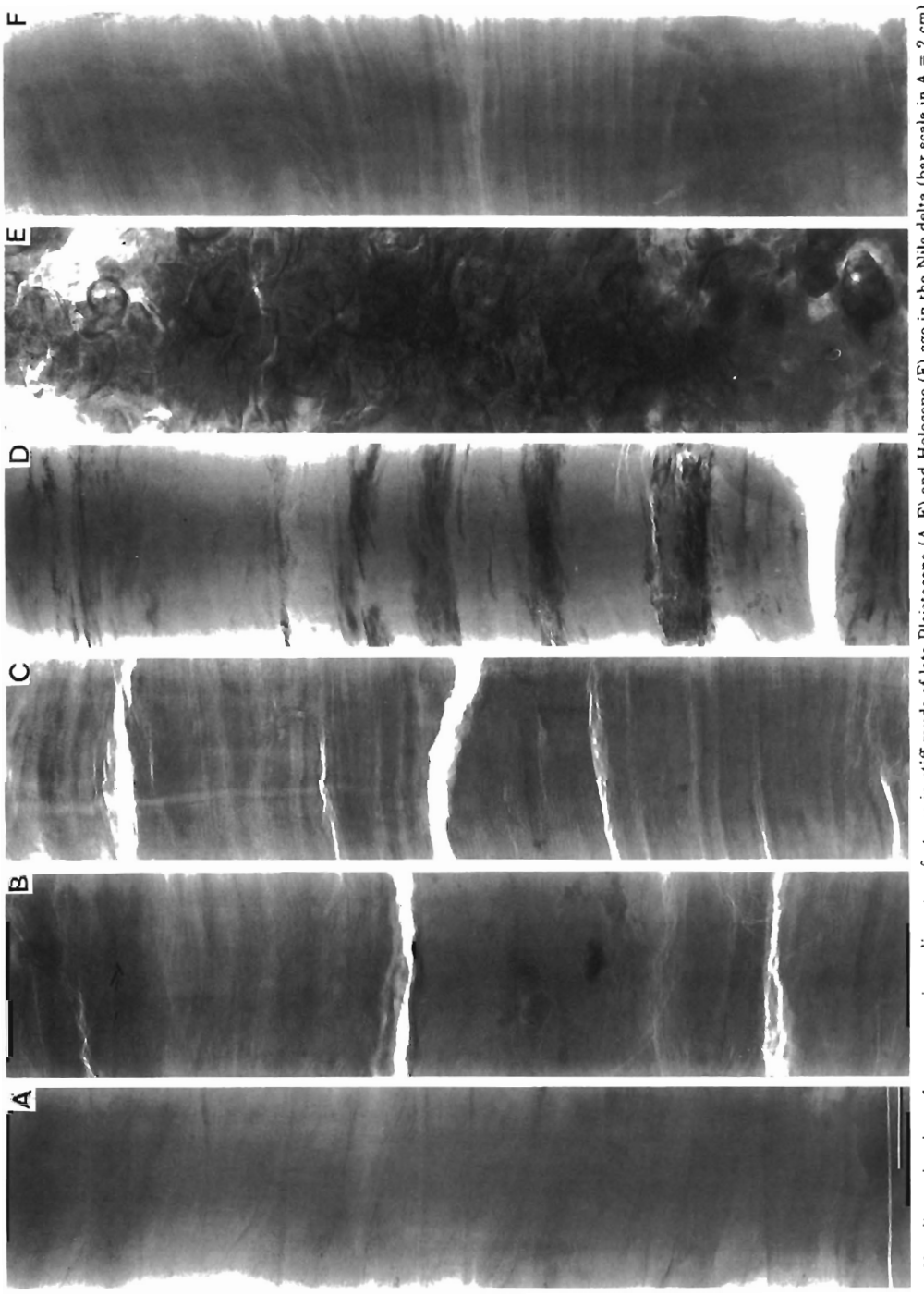

Figure 6. X-radiograph prints of representative sedimentary features in stiff muds of late Pleistocene (A–E) and Holocene (F) age in the Nile delta (bar scale in A = 2 cm). A, cross-bedding and climbing ripple stratification (core S-81, section V, depth ~9.5 m); B, sinuous lamination and randomly distributed large calcareous nodules (core S-73, section IX, depth ~13.5 m); C, horizontal lamination (core S-50, section XIII, depth ~24.3 m); D, jarosite lenses (appear as dark horizons), always in association with plant matter (core S-33, section XIV, depth ~21.3 m); E, mollusc-rich coquina (complete and separate valves) in mud matrix (core S-28, section X, depth ~27.5 m); F, horizontal and inclined lamination (core S-86, section IX, depth ~12.0 m).

sands. The color (dark brown to brownish grey; Figure 7B) of mud forming sequence II, differs markedly from that of sequence I (yellowish brown).

Unit D is medium dark grey (N4) to dark grey (N3) mud with a moderate to high proportion of organic matter. It generally forms the base of sequence II, and ranges in thickness from 0.4–2.6 m. Organic matter is usually concentrated in well-defined layers from ~0.5 to 1.0 cm thick (Figure 7C). The thin organic-rich laminae suggest considerable compaction since deposition. Jarosite-rich [$KFe_3(SO_4)_2(OH)_6$] muddy lenses, identified by X-ray diffraction, are usually 0.2–1.5 cm thick (Figure 6D), and occur as distinct yellowish brown horizons interbedded in mud. Gypsum nodules of small size (~0.2 cm in diameter) are also sporadically dispersed throughout the unit.

Unit E is a brownish grey (5YR 4/1) mud that usually lies above unit D; it ranges in thickness from 0.1–3.6 m. Most diagnostic are randomly disseminated gypsum nodules (minimum diameter, ~0.1 cm; maximum diameter, ~4.0 cm) and layered gypsum crusts (0.5–2.0 cm in thickness; Figure 7B and C), specks of Fe/Mn oxide, and thin, rusty colored plant-rich lenses. Oxidized root traces are observed in some sections. Mud cracks, usually ~0.5 cm in width and ~0.8 cm in length, are present at the top of this unit. Repetitions of layered gypsum nodules, often with tooth-like crystals, occur locally. The lithologic boundary between units D and E is gradational. Unit C, a light brown sandy mud, caps unit E, and forms the top of sequence II.

The association of sedimentary features in sequence II records fluvial sediment dispersal in a flood basin, but accumulation appears to have been more distal from terrigenous river channels than sequence I. On the basis of 11 radiocarbon dates, deposition occurred during two periods: ~34,000–21,000 years BP, and ~13,000–12,000 years BP.

Sequence III, Shell-Bearing Stiff Mud

This subfacies is formed by units F, G and C, and occurs in 6 cores. Sediment color is generally brownish grey. The sequence has a maximum thickness of 1.8 m, and is usually underlain by late Pleistocene shallow marine sands. This subfacies is distinguished from the other three sequences by an abundance of molluscan shells, either complete or as individual valves (Figures 6E and 7D).

Unit F, forming the base of the sequence, is a brownish black (5YR 2/1) locally organic-rich mud with some dispersed shells; it ranges in thickness from 0.7–0.8 m. Randomly distributed calcareous nodules occur throughout, and poorly defined horizontal lamination is observed. Minor proportions of brackish to marine microfossils, such as foraminifera and ostracods, are also present.

Unit G is a dark grey (N3) mud, much richer in shell, which commonly lies above unit F and ranges in thickness from 0.3–0.6 m. The fauna (such as in S-28) comprises gastropods, including *Cerithium (Thericium) vulgatum* (Brugière), *Columbella rustica* Linneo and *Hinia costulata* (Renieri) and pelecypods, including *Cerastoderma glaucum,* and *Tellina* sp. Foraminiferal and ostracod tests are also common. Randomly dispersed calcareous nodules are observed, and in some units a few layered calcareous nodule horizons are also noted. Plant material is locally abundant. The lithologic contact between units F and G is sharp. Unit C, a light brown sandy mud generally caps unit G, and forms the top of sequence III.

The association of sedimentary features and fossils in sequence III indicates brackish to salt water conditions. On the basis of 4 radiocarbon dates, it appears that deposition occurred during two periods: ~27,000–19,000 years BP and ~11,000 year BP.

Sequence IV, Plant Debris-Bearing Stiff Mud

This subfacies is formed by units H, I and C, and occurs in 6 cores. Sediment color is generally greyish black. This sequence has a maximum thickness of 2.4 m, and basal unit H is usually directly underlain by quartz-rich stained alluvial sand of late Pleistocene age.

Unit H, the lower layer, is a dark grey (N3) to greyish black (N2) mucky mud (1–15% plant matter), and ranges in thickness from 0.1–1.4 m. Randomly distributed calcareous nodules occur throughout. Weakly developed horizontal lamination and rusty colored sandy lenses also occur.

Unit I is a greyish black (N2) muck (15–45% plant debris) with thin mucky peat layers rich in plant matter (Figure 7E). It lies above unit H and ranges in thickness from 0.2–0.5 m. Calcareous nodules occur sporadically. In some cores, fresh water gastropods, ostracods and sponge spicules are present, and are mixed with minor proportions of brackish water microfossils. The litho-

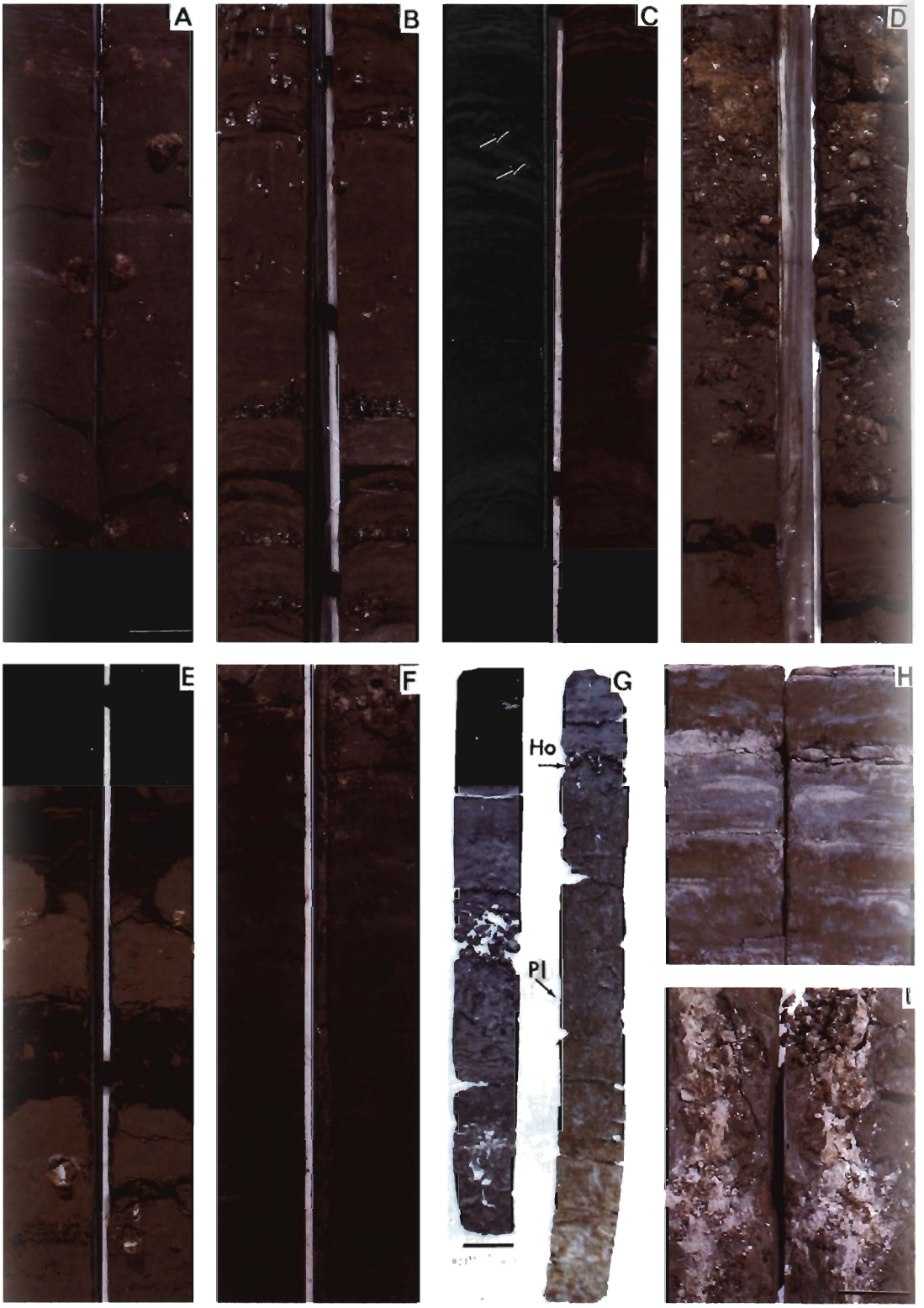
A
B
C
D
E
F
G
Ho
Pl
H
I

logic contact between units I and H is sharp. Unit C, a yellowish brown sandy mud caps unit I and forms the top of sequence IV.

The association of sedimentary features and floral and faunal content forming sequence IV suggests fresh water-dominated marsh conditions. The only 2 available radiocarbon dates indicate deposition from ~35,000–27,000 years BP.

COMPOSITION OF SEQUENCES

In addition to the gross lithologic attributes summarized above, composition of the sand-size fraction and clay mineralogy can be used to further differentiate the major Nile delta stiff mud subfacies (sequences I to IV) of late Pleistocene age. Of particular value in this respect are the point-count sand compositional data for 214 mud core samples and clay mineral data for 56 additional samples specifically selected from the four above-defined sequences (Tables 1 and 2, respectively).

Sand-Size Fraction

The 214 samples examined for sand-size composition were derived from: sequence I = 129 samples; sequence II = 27 samples; III = 22 samples and IV = 36 samples. Petrographic data from the four sequences are subdivided and plotted as five groups by statistical box calculation method (Figure 8). Plots show that all samples are dominated by light minerals, primarily quartz. Calcareous nodule, gypsum nodule, shell and plant debris are the most diagnostic sand-sized components used to distinguish subfacies (Table 1). Also important are the proportions of sand relative to silt and clay, and some of the associated components (described below). Two of the five groups are calcareous nodule-dominated, and are differentiated on the basis of different relative percentages of calcareous nodules and unidentified carbonate particles. These two carbonate subtypes (Ia and Ib in Figure 8A and B) are considered variants of one major subfacies, calcareous nodule-bearing stiff mud.

Calcareous Nodule-Bearing Stiff Mud (Two Variants)

Sediment is composed mostly of silt and clay, but the proportion of sand is sometimes quite high (to ~50%). In one variant of this facies (Ia), calcareous nodules (including minor proportions of aggregate) and light minerals are the diagnostic compositional components (Figure 8A). The median value of calcareous nodule content is ~12%, and the maximum value is 33%. Minor amounts of fresh water gastropod fragment, ostracod and sponge spicule occur. Heavy mineral, mica, glauconite/verdine, lithic fragments, plant debris and unidentified carbonate particle constitute the accessory suite.

A second variant (Ib) is characterized by a higher proportion of unidentified carbonate particle, with a median value of ~8% and maximum of 78% (Figure 8B). Sections of this variant occur primarily in the northwesternmost Nile delta sector, in cores S-77 to S-85 (Figure 1). In that sector, Nile delta terrigenous (largely quartz) dispersal is reduced and carbonates dominate (EL-FAYOUMY *et al.*, 1975; STANLEY, 1989; STANLEY and HAMZA, 1992; WARNE and STANLEY, 1993). Of the two, variant Ia, distinguished by its carbonate nodule content, is more widely distributed in cores across the northern Nile delta than variant Ib.

Gypsum Nodule-Bearing Stiff Mud

Sediment is composed mostly of silt and clay, but sometimes includes a substantial proportion of sand (~30%), although in lower amounts than in Type I. Gypsum is the diagnostic component: median percentage in the sand-size fraction is ~1%, and maximum extreme values range from 35 to 80% (Figure 8C). Mica content (~3%) is somewhat higher than in other stiff mud types. In addition, a small proportion of fresh water gas-

←

Figure 7. Split core sections of representative stiff mud types examined in this study (bar scales = 5 cm). A–E, late Pleistocene in lower Nile alluvial plain: A, sequence I, with randomly distributed calcareous nodules (core S-47, depth ~34.3 m from core top); B, sequence II, showing both randomly and layered gypsum nodules (core S-35, depth ~30 m); C, sequence II, showing dark organic-rich lamination and (arrows) Fe/Mn oxides (core S-33, depth ~21.2 m); D, sequence III, showing concentration of shell (core S-28, depth ~27.5 m); E, sequence IV, showing two plant-rich layers and randomly distributed calcareous nodules (core S-34, depth ~24.8 m). F, Holocene in central Nile delta, with layer of calcareous nodules in upper core section (core S-86, depth ~4.5 m). G, lower plain in Yangtze delta, showing mottled oxidized stiff mud of late Pleistocene age (Pl), underlying soft grey muds of Holocene (Ho) age (core Y-1, base of core section at lower right is at a depth ~29.0 m). H, I, late Pleistocene in lower plain of Mississippi delta: H, weakly developed horizontal lamination in oxidized mud, interbedded with sand lenses (core 5U-DAV, depth ~22.0 m); I, carbonate filling crack (core WLW-21UT, depth ~18.0 m).

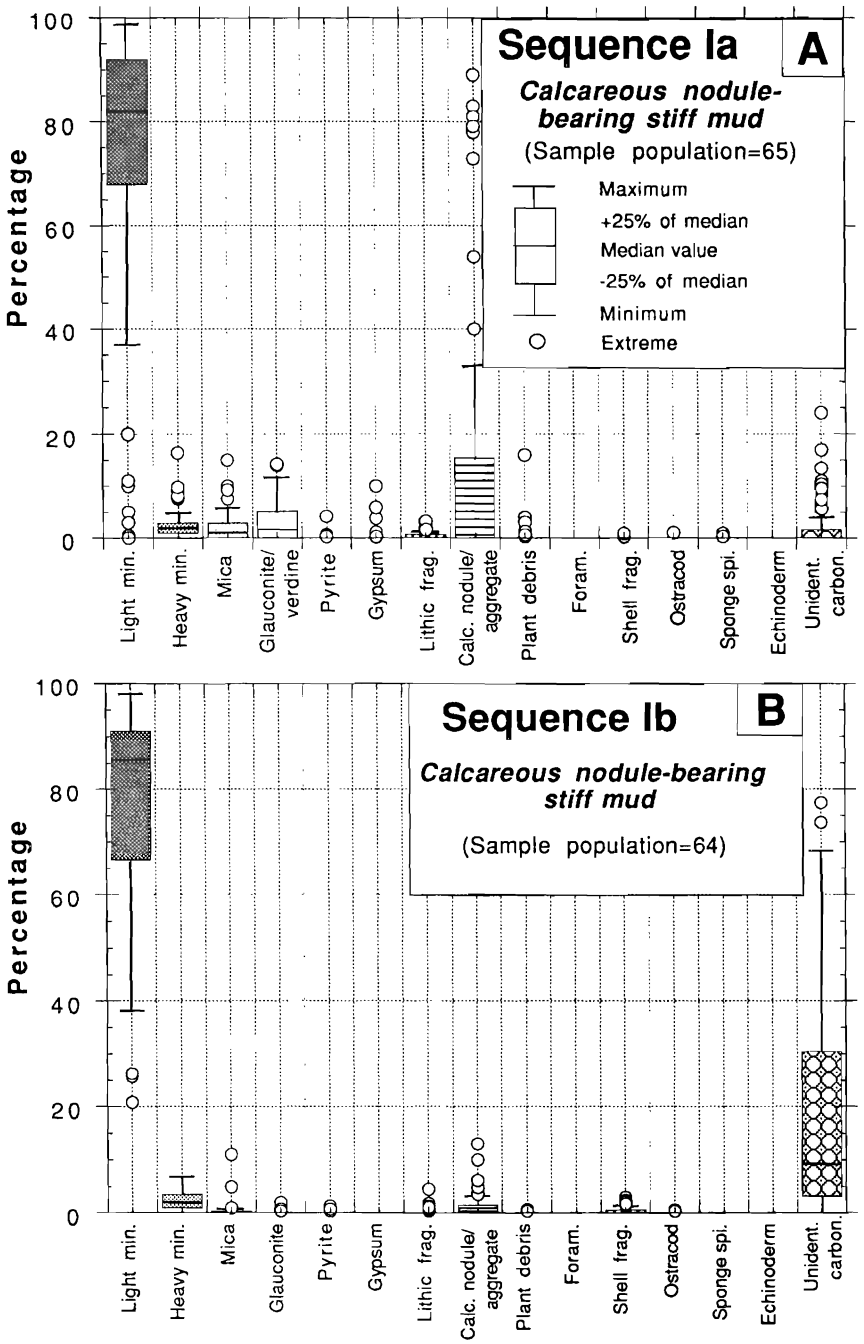

Figure 8. Plots based on box calculation showing trends of sand-size compositional components in 4 Nile major stiff mud sequences (I to IV, see Figure 5).

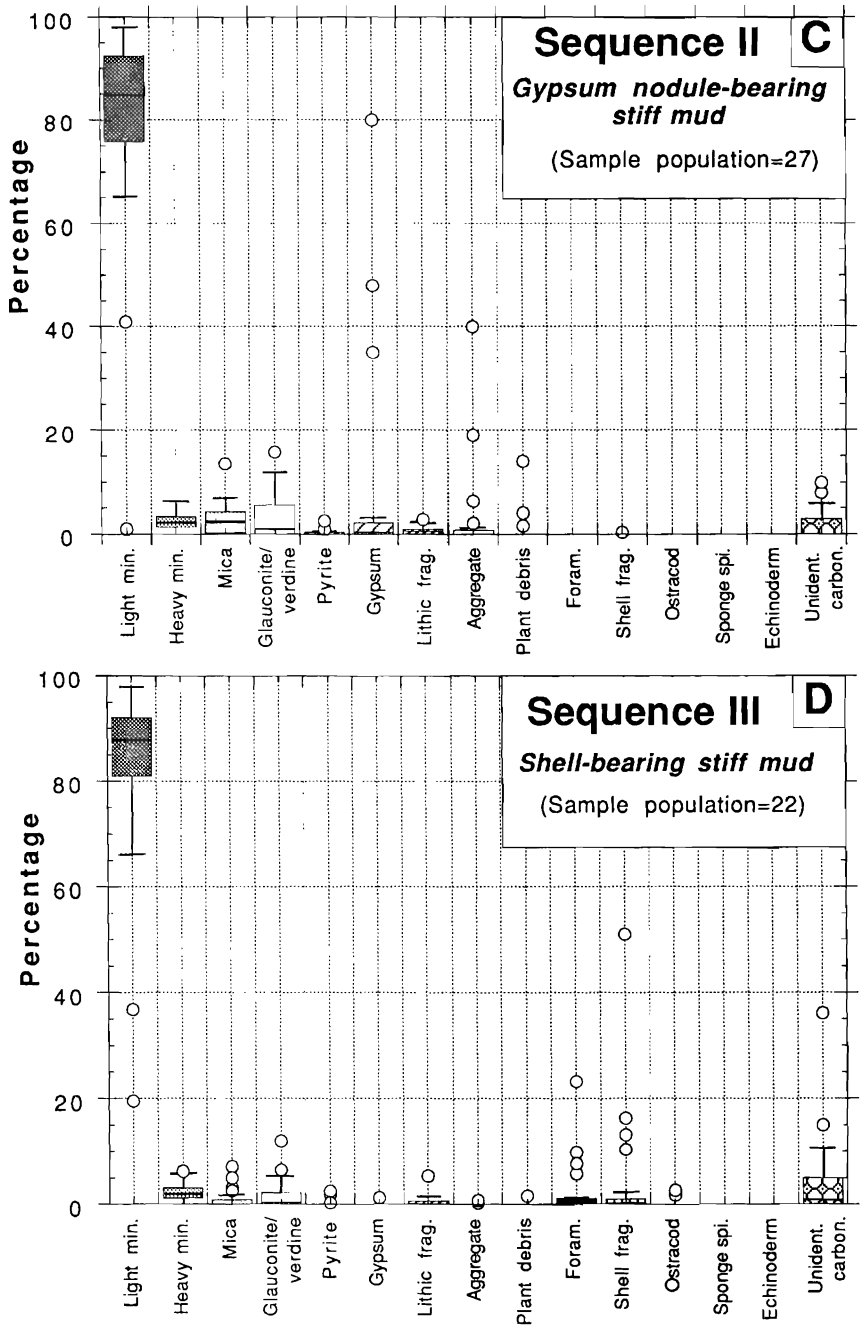

Figure 8. *Continued.*

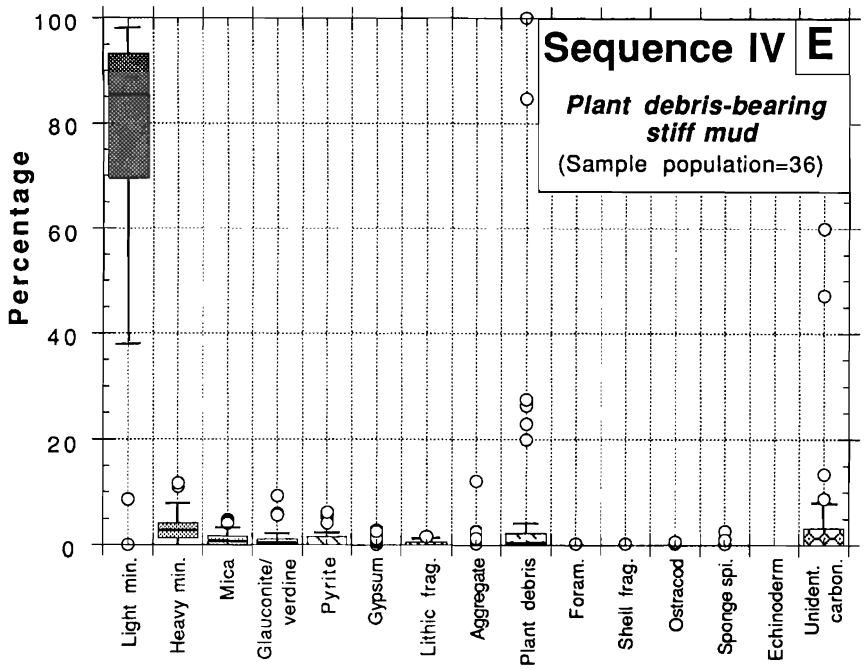

Figure 8. *Continued.*

tropods is present. Heavy minerals, glauconite/verdine, lithic fragments, aggregate, plant debris and unidentified carbonate particles constitute the accessory suite.

Shell-Bearing Stiff Mud

Sediment is composed mainly of silt and clay; of the four types, it has the lowest proportion of sand. Mollusc shells are diagnostic and in the sand-sized fraction are usually fragmented; content ranges from 0.5 to 50% (Figure 8D). It is of note that a relatively high percentage of fossils (*e.g.*, foraminifera, ostracod and pelecypod) are of taxa generally associated with brackish to open marine conditions. Pyrite is also a diagnostic component. As in stiff mud types I and II, light minerals are the predominant constituent, but quartz is less iron-stained. Heavy minerals, mica, glauconite/verdine, lithic fragments, plant debris, and unidentified carbonate particles constitute the accessory suite.

Plant Debris-Bearing Stiff Mud

Sediment is composed mainly of silt and clay; the proportion of sand is intermediate between types II and III. Plant debris content, with median to maximum values ranging from 1 to 5% (with extreme values for some samples ranging from 20 to 100%), tends to be higher in this (Figure 8E) than in the other three types. Many of the plant debris-bearing stiff muds could be termed mucky mud and muck, with 1–15% and 15–45% plant matter content, respectively. Comparable vegetal-rich muds were described in much younger Holocene sections of the lower Nile delta plain by Howa and Stanley (1991). Also of note are significant proportions of pyrite. Foraminifera, fresh water gastropod, ostracod and sponge spicule occur locally. Heavy minerals, mica, glauconite/verdine, lithic fragment, aggregate and unidentified carbonate particles constitute the accessory suite.

Clay Mineral Composition in Sequences

Since silt and clay are the dominant fractions in stiff mud facies, it is of value to consider the proportions of major clay minerals associated with the four major sequences. Smectite, kaolinite and illite, in order of importance, form the clay mineral suites in all core sequences. Values are determined on the basis of XRD analyses (using

peak height) of 56 samples in 37 cores (averaged data in Table 2): sequence I = 40 samples; II = 10 samples; III = 4 samples; IV = 2 samples. Proportions of each clay mineral differ in each sequence.

Smectite averages 50% in sequence I, 48% in II, 44% in III and 31% in IV.
Kaolinite averages 34% in sequence I, 38% in II, 35% in III, and 50% in IV.
Illite averages 16% is sequence I, 14% in II, 21% in III and 19% in IV.

In summary, the four major stiff mud subfacies underlying the Nile delta can be generally distinguished when compositional attributes of both sand-size and clay mineral fractions are considered together. It is encouraging that the four major sequences in a large number of cases, can be identified on the basis of petrographic analysis of small samples alone.

DISTRIBUTION IN TIME AND SPACE

General

The temporal and spatial distributions of late Pleistocene Nile stiff muds are shown in Figures 9A–F and 10. The maps reveal that this facies in the 42 Smithsonian cores is discontinuous and unevenly distributed across the northern delta plain (Figure 9A): in the northeastern delta, stiff mud occurs in 7 cores located south of Manzala lagoon; in the north-central Nile delta, in 24 cores between the Damietta and Rosetta branches; and in the northwestern delta, in 9 cores in the Alexandria and Maryut lake area, and 2 south of Idku lagoon. Stiff muds may underlie Manzala lagoon. However, none are reported in several long cores described by ATTIA (1954). The limited number of Smithsonian cores in and immediately adjacent to the lagoon did not penetrate sufficiently into the late Pleistocene sections (Figure 10).

A mud layer herein refers to an individual, discrete mud section which may comprise one or more sequences. Layers range in thickness from 0.2 to ~10 m, and are usually 2 to 3 m thick. The number of layers and their thickness in the 42 cores is shown in Figure 9D. Stiff mud occurs as a single layer in most cores (Figures 9D, 10). Exceptions are 6 cores in the north-central Nile delta (S-28, S-36, S-38, S-43, S-46, and S-54; Figure 9D) with 2 stiff mud layers, and 1 core (S-81) in the Maryut lake region, in the northwestern Nile sector, with 3 stiff mud layers.

Stratigraphic profiles show that all mud layers occur as geographically restricted lithosomes which interfinger with and are separated by the more widespread late Pleistocene iron-stained sands of alluvial, wind-blown, and shallow marine origin. Muds are topped by late Pleistocene to early Holocene transgressive sand or by Holocene delta sand and mud (Figure 10). The depth of layers below present ground surface varies regionally, from ~3 to 35 m. Their depth in cores positioned further to the south (profile B-B′ in Figure 10) is generally 5 to 10 m shallower than in cores to the north (profile A-A′ in Figure 10).

Mud layers are concentrated in 14 distinct geographic zones, ranging in area from ~10 to 800 km^2. Most of these lithosomes display an oval or elongate pattern which varies in orientation in different parts of the delta (Figure 9E): a NE–SW elongation in the northeastern sector; a NNE–SSW elongation in the Baltim-Gamasa region and NNW–SSE elongation in the Burullus lagoon region in the north-central sector; and a NW–SE elongation in the northwestern sector. In the Maryut-Alexandria region the lithosome has an irregular configuration, roughly paralleling the outline of Maryut lake and high-relief carbonate ridges (Figure 9E). The ridges were emergent during deposition of the stiff mud sequences.

Spatial Distribution of Sequences

It is recalled that late Pleistocene stiff muds are subdivided into 4 major sequences (I–IV in Figure 5) which are formed by various associations of 9 depositional units (A to I). A total of 148 units are mapped in the 50 stiff mud layers in the 42 cores (Figure 9B).

The most common stiff mud units are A (22%), B (28%) and C (26%) (Figure 9B). Sequence I (calcareous nodule-bearing stiff mud), composed mainly of units A and B, is clearly the dominant subfacies (Figure 9C). Second in importance is sequence II (gypsum nodule-bearing stiff mud), which is mainly composed of units D (3%) and E (8%). Sequences III (shell-bearing stiff mud) and IV (plant debris-bearing stiff mud), mainly composed of units F (3%), G (3%), H (4%) and I (2%), comprise only a minor proportion of the lithofacies.

Lithofacies forming the 14 lithosomes are shown on the basis of the dominant sequence in each stiff mud section (Figure 9F). Sequence I, calcareous nodule-bearing stiff mud, most commonly forms these lithosomes. Where present (in 9 out

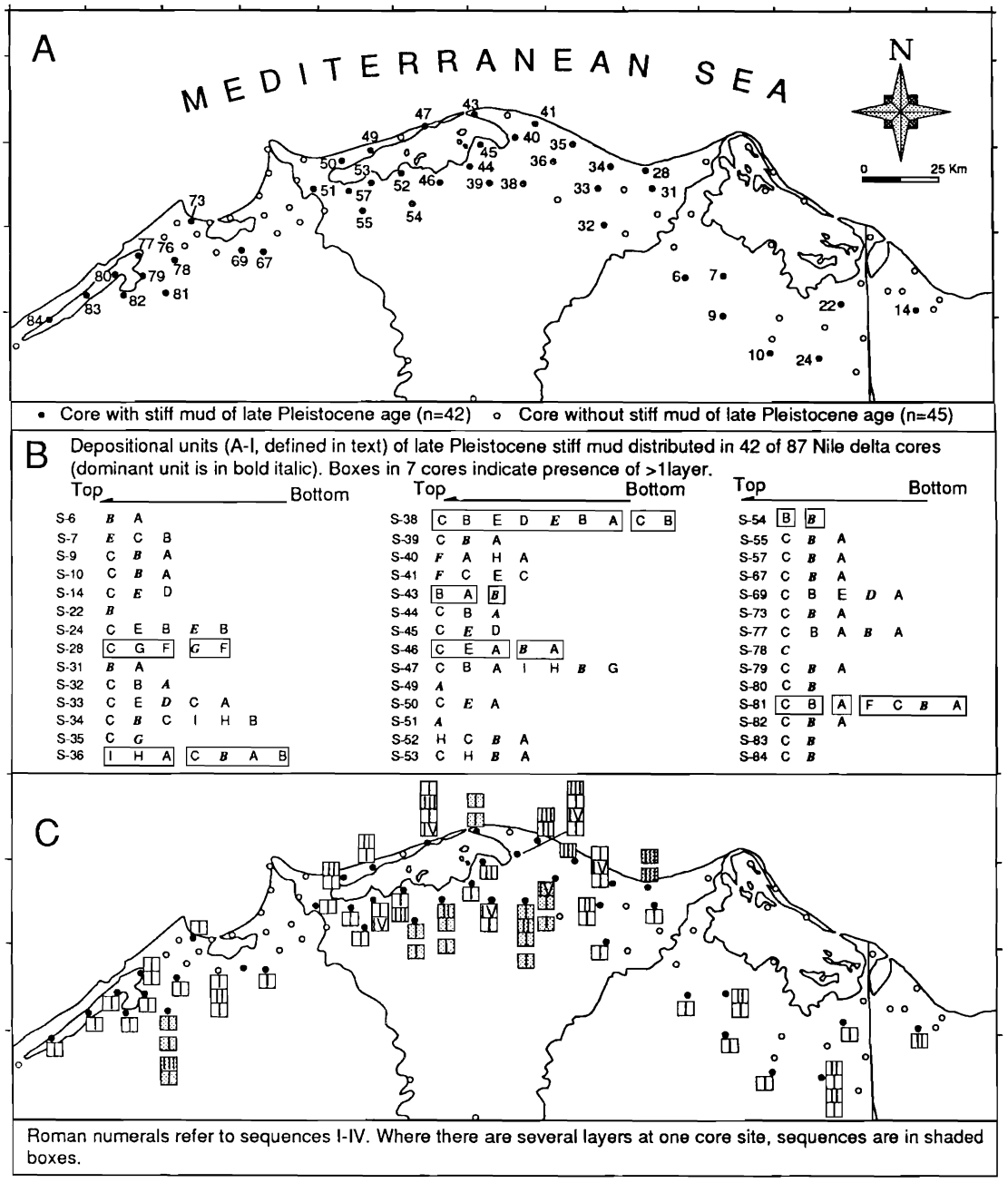

Figure 9. Series of maps of northern Nile delta showing: (A) position of 42 (of 87) cores with late Pleistocene stiff mud; (B) 148 depositional units forming stiff mud layers in 42 cores; (C) distribution of stiff mud sequences I to IV, and cores containing more than one stiff mud layer (shaded boxes); (D) thickness and number of stiff mud layers; (E) isopach configuration of 14 stiff mud lithosomes; and (F) distribution of the four stiff mud subfacies sequences in the 14 lithosomes.

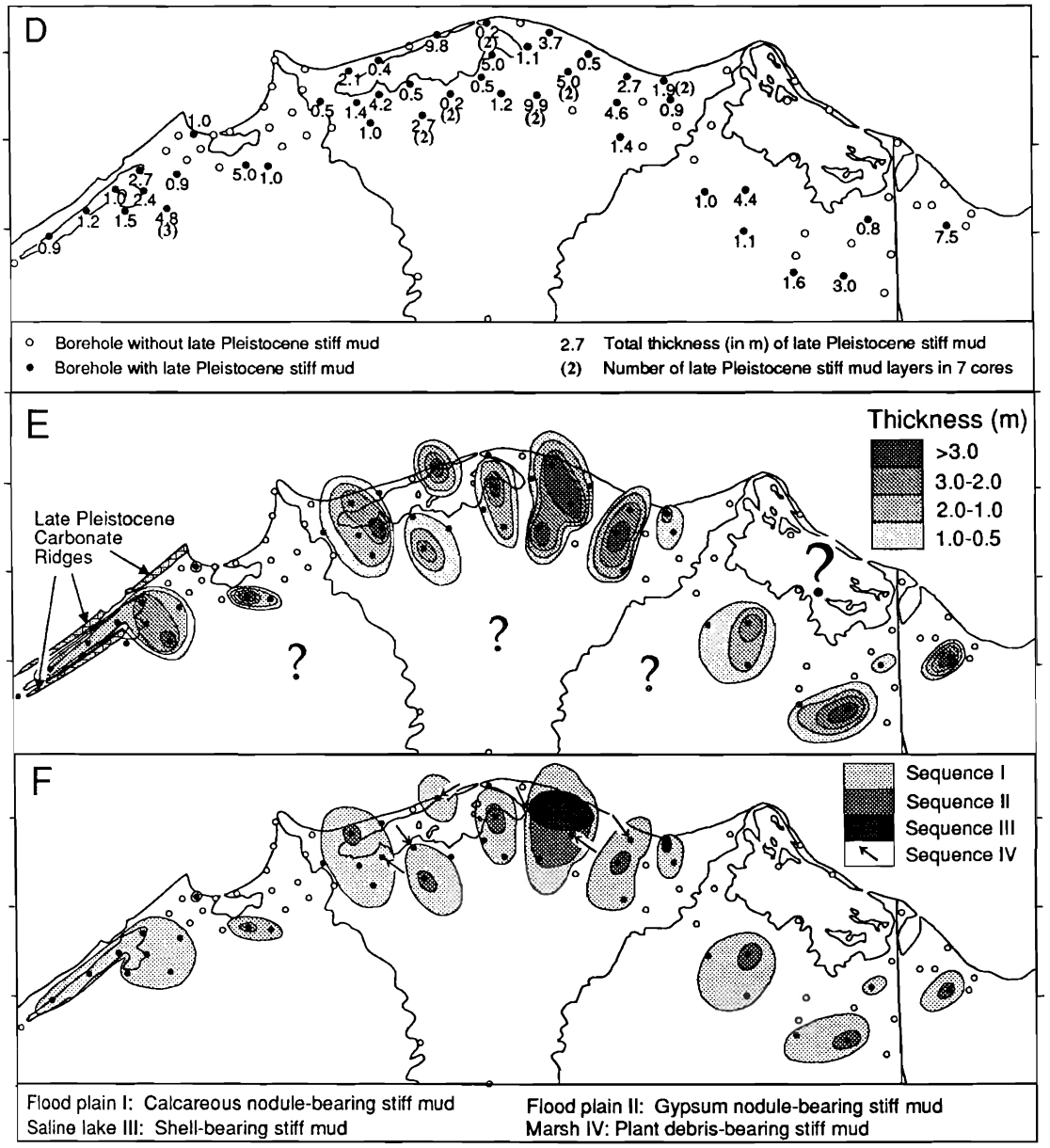

Figure 9. *Continued.*

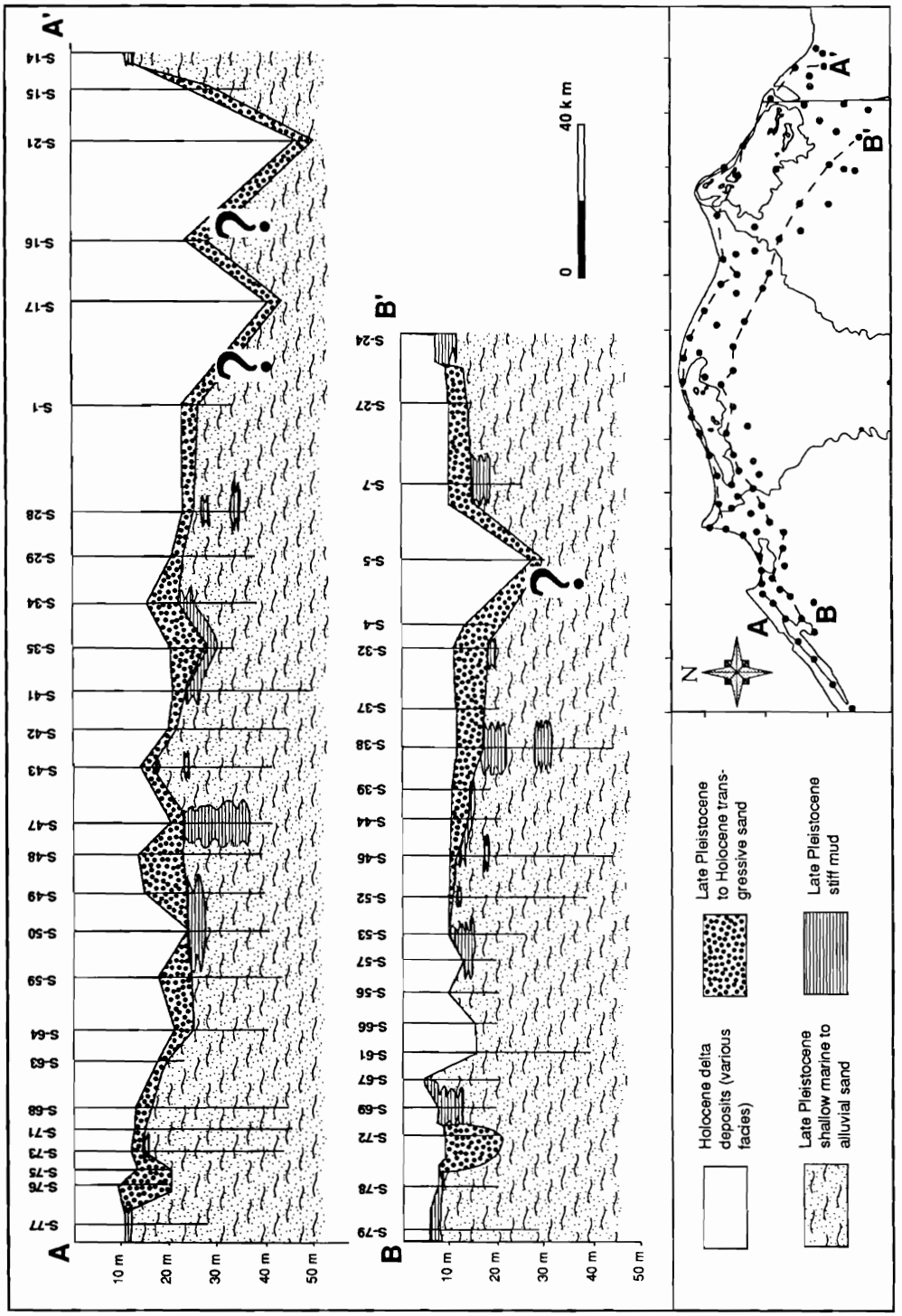

Figure 10. Two coast-parallel stratigraphic profiles showing the distribution of Holocene and late Pleistocene sections, including stiff mud layers.

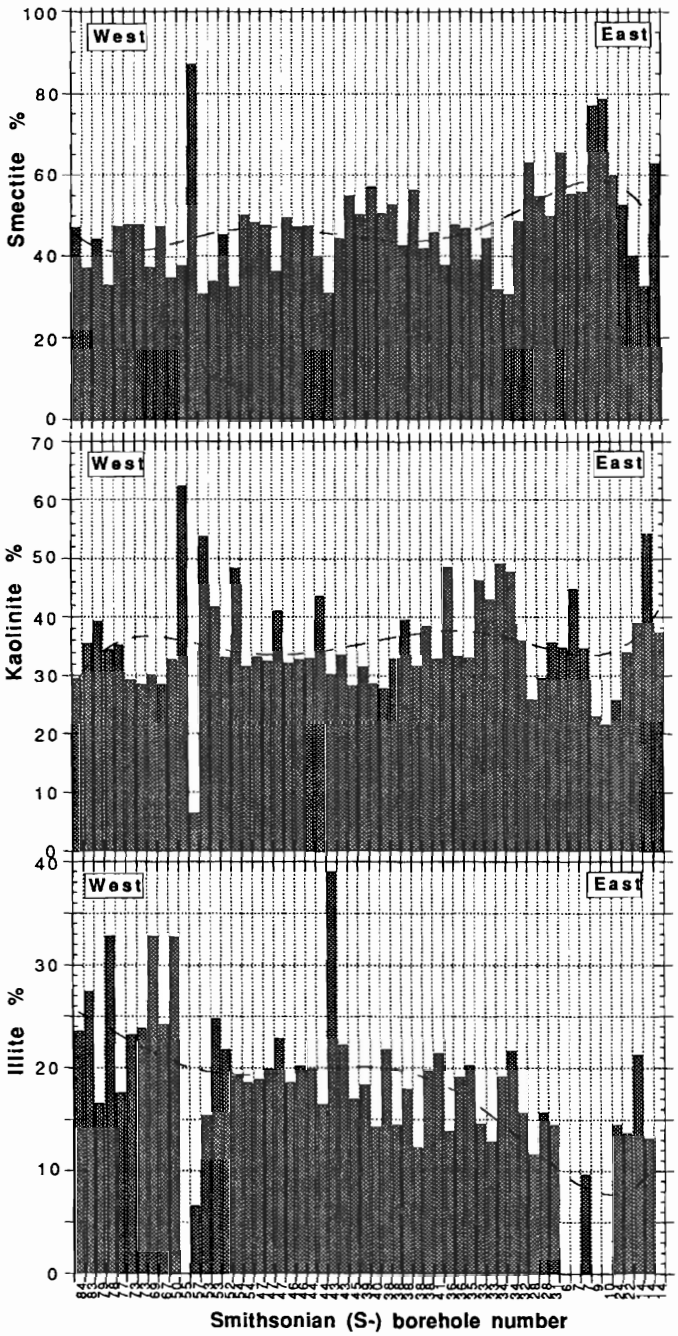

Figure 11. Distribution, from east to west, of clay minerals in stiff mud layers.

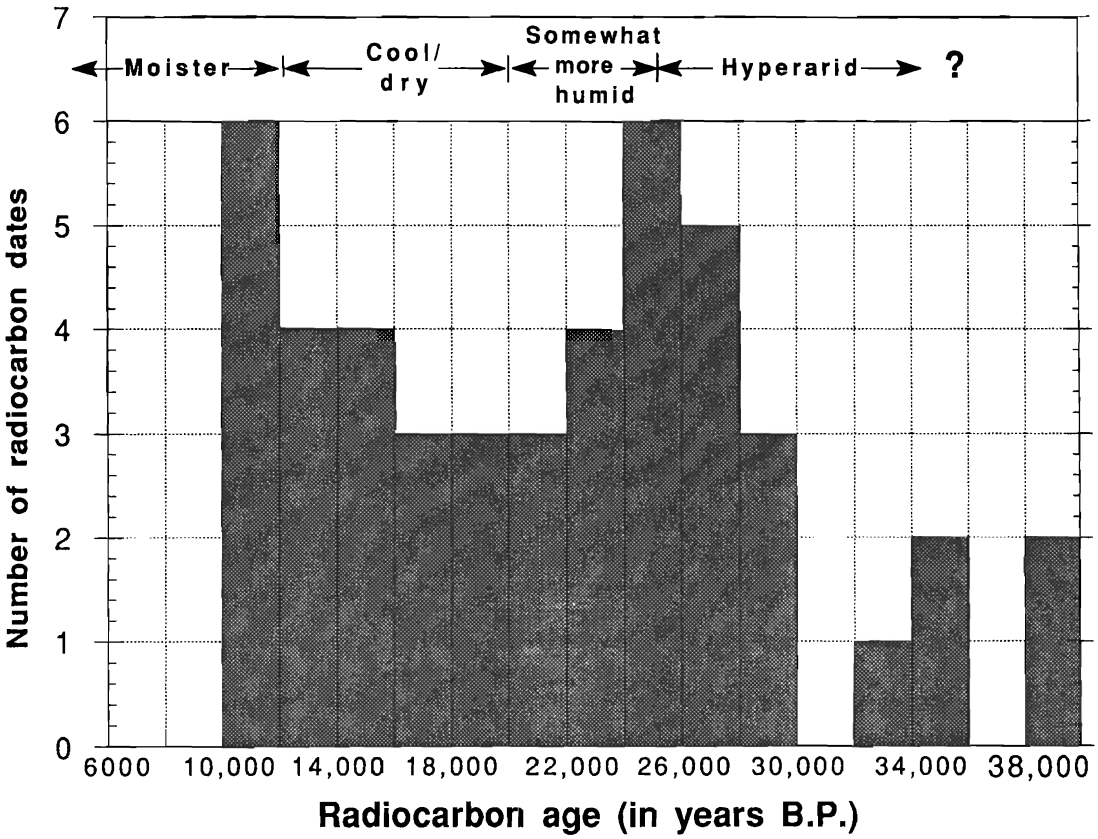

Figure 12. Histogram showing frequency of radiocarbon-dated stiff mud samples versus age in years BP.

of the 14 lithosomes), sequence II, gypsum nodule-bearing stiff mud, always appears at or near the center of the lithosomes dominated by sequence I (Figure 9F). Sequence III, shell-bearing stiff mud, occurs mainly in the Baltim to Gamasa region. Sequence IV, plant debris-bearing stiff mud, is localized in the north-central delta (in cores S-34, S-36, S-39, S-40, S-57 and S-53).

Regional Distribution of Clay Minerals

The relative percentage of clay minerals is shown for each core site, from east to west (Figure 11).

Smectite is the dominant clay mineral, with an overall average percentage approximating 47%, for all 56 samples examined. Smectite content is considerably higher (average ~58%) in cores recovered east of the Damietta branch, and decreases (average ~45%) west of the Rosetta branch in the northwestern sector.

Kaolinite proportions are fairly constant from east to west, with an average of ~32%.

Illite values average about 20%; in contrast to smectite, illite increases from ~10% in the east to ~25% in the west.

Temporal Distribution of Stiff Mud

A total of 46 radiocarbon dates were obtained from 36 layers in 33 cores (MEDIBA, 1992). Dates range from >38,000 to ~11,000 years BP (Figure 12). A histogram showing age versus number of all dated samples indicates that deposition was episodic but time-related, generally occurring at: >34,000, ~28,000–22,000, and ~16,000–>10,000 years BP.

The relative abundance of different sequences also varies over time. Sequence I accumulated during most of the period considered, *i.e.*, from >38,000 to ~11,000 years BP; sequences III and

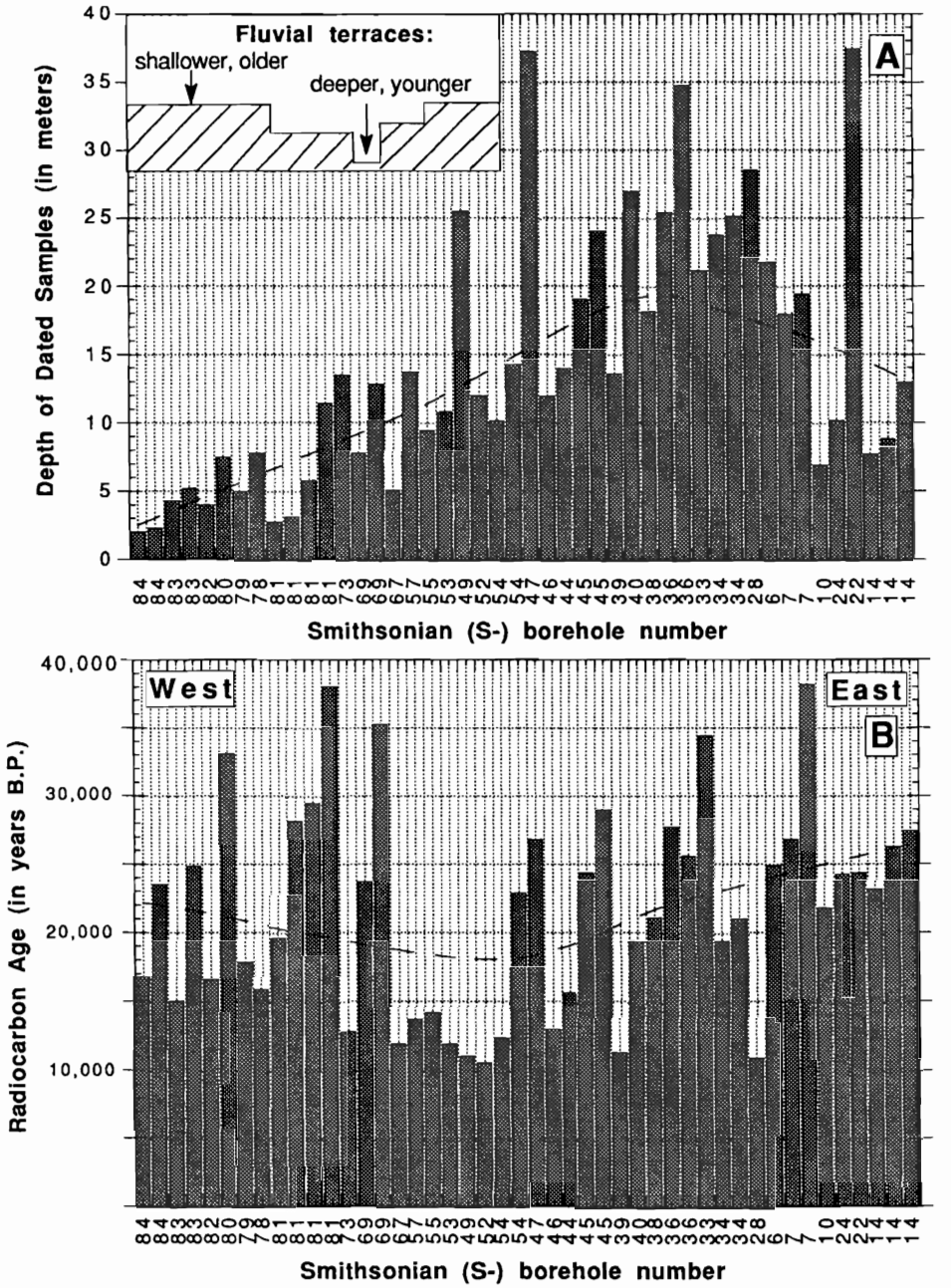

Figure 13. Histograms showing, from east to west, Smithsonian boreholes versus (A) depth of radiocarbon dated samples, and (B) age of radiocarbon dated samples (dashed lines denote averaged values). Data reveals the offset between depth and age of stiff mud: deeper layers tend to be younger, and shallower ones are usually older. This phenomenon is related to a migrating channel-fluvial terrace origin (inset).

IV appear more rarely during this period. Sequence II occurs preferentially between ~34,000 and 21,000 years BP.

The depth of dated samples is shown in Figure 13A (ground level of all cores is near sea level). A calculated curve shows average depth of radiocarbon-dated samples, from east to west. This curve indicates that dated mud layers in eastern Manzala lagoon sector and in Maryut lake region lie, for the most part, at only 3 to 10 m below the present surface. The average depth of dated samples increases to ~20 m in the Burullus-Gamasa region in the north-central delta (in cores S-28 to S-47; Figure 13A).

A curve showing average age, calculated for the radiocarbon data set (Figure 13B), indicates a general inverse relationship between depth of a mud layer below ground surface and its radiocarbon age. In the case of many samples, the deeper the stiff mud layer, the younger its age (*cf.* Figure 13A and B). It is noted that the deepest average stiff mud sequences in core localities (in the vicinity of S-38) and average youngest dated sample (in S-52) do not occur at the same geographic location (Figure 13A and B).

There is also some relation between the clay mineral content and age. The proportion of smectite is highest, and kaolinite decreases, in stiff mud dated at about 26,000 to 24,000, 22,000 to 20,000, and 14,000 to 12,000 years BP. These changes in clay mineral content occur during periods of predominant stiff mud accumulation (Figure 12). Illite does not show a distinct time-related trend.

DEPOSITIONAL ORIGIN OF STIFF MUD SEQUENCES

The petrology of the four major sequences (Figure 5), and their distribution in time and space (Figures 9–13), serve to interpret the origin of the Nile stiff muds.

Sequence I deposits accumulated during a time when sea level was much lower than at present (CURRAY, 1965; MÖRNER, 1971; LIGHTY *et al.*, 1982; FAIRBANKS, 1989), the sampled area was subaerially exposed, and the coastline was positioned much farther to the north (ABDEL WAHAB and STANLEY, 1991:Figure 5). This subfacies was emplaced by flood waters, carrying admixtures of clay, silt and sand. Locally dispersed pebbles in some unit A muds record powerful flow. These sediments were transported by minor overflow channels or they breached and overtopped river channel levees and were released in adjacent proximal depressions. Deposition occurred at a proximal site, away from plant growth and close to fluvial dispersal of terrigenous sediment. Sediment was released in quiet water bodies, as indicated by fining-up sequences (units A and B). The shallow, discontinuous depressions were analogous to some modern low-relief depressions along the Nile valley that are periodically flooded (*cf.* BUTZER, 1976, p. 17). After floodwater in these depressions evaporated, sediments were subaerially exposed during most of the year in a sparsely vegetated semi-desert setting. These depositional conditions and the effects of subaerial exposure to arid conditions are particularly well recorded by unit B deposits which contain oxidized patches, iron-stained sand lenses in mud layers, calcareous nodules, caliche structures and other features indicative of evaporation, transpiration and soil infiltration. These features suggest that the water table fluctuated with alternating wet and dry seasons (*cf.* REINECK and SINGH, 1980; WUNDERLICH and ANDRES, 1991; GUSTAVSON, 1991). Calcareous crusts formed on a surface that is gradually aggrading. Mudcracks record a break in deposition and subaerial exposure affected by alternating wet and dry periods (KOMORNIK *et al.*, 1970; GUSTAVSON, 1991). X-ray diffraction analysis of calcareous nodules indicates a low Mg ion chemical composition recording a fresh water derivation (*cf.* KLAPPA, 1983; SCHOLLE *et al.*, 1983). Sandy mud (unit C), buried the underlying oxidized yellowish grey mud surface (unit B). This admixture strongly suggests wind-blown sands (STANLEY and CHEN, 1991) deposited on a muddy alluvial plain. A similar wind storm process may be observed on the modern Nile delta plain (WEST *et al.*, 1979; ALI and WEST, 1983; STANLEY *et al.*, 1992) and in depressions bounding the Nile valley. Thus, the overall association of petrologic features indicates that sequence I is a type of inland sebkha, or playa, deposit which accumulated in a series of small to modest sized, seasonally flooded depressions in proximity to Nile channels. Dunes and related eolian deposits periodically accumulated during dry seasons.

Sequence II, usually associated with sequence I, is also interpreted as a deposit seasonally introduced by Nile floods in inland depressions that have been exposed to arid, evaporative conditions. Some differences with sequence I include darker color with sandy specks, generally finer grain size, and the presence of laminated organic matter,

dispersed gypsum nodules and some jarosite lenses in the lower part (unit D). Jarosite formation is secondary, and perhaps related to transformation from plant debris; vegetal material commonly occurs just above or below jarosite lenses. It has been suggested that such transformation to jarosite requires arid climatic conditions (FRYE, 1981). This is followed upward by layered gypsum crusts (unit E). Some layered gypsum, like layered calcareous nodules in sequence I, record vertical shifts in the water table. More likely, layered gypsum evaporites are crusts indicative of evaporative phases, following precipitation of the carbonate, as water level was lowered during dry seasons in the study area. Locally present oxidized root traces may indicate capillary function during digenetic processes (WEST *et al.*, 1979; ALI and WEST, 1983; GUSTAVSON, 1991). This petrologic association is similar to deposits in some modern inland sebkhas (*cf.* GLENNIE, 1970; MABBUTT, 1977) and suggests accumulation in somewhat deeper, more central sectors of playas (*cf.* WATSON, 1979). These were more distal relative to flood channels than sequence I depositional sites. As in the case of sequence I, the subaerially exposed mud-cracked and gypsum crust surfaces are usually covered by wind-blown sandy mud, suggesting proximity to dunes.

Sequence III is much less common in terms of thickness and aerial extent than either I and II. This stiff mud subfacies is associated with these two sequences and located in the center of two lithosomes (Figure 9F) positioned in the north-central delta, between Baltim and Gamasa. This subfacies is in fact comparable, in a number of aspects, to Nile delta lagoon facies of Holocene age (COUTELLIER and STANLEY, 1987; ARBOUILLE and STANLEY, 1991; CHEN *et al.*, 1992; STANLEY *et al.*, 1992; LOIZEAU and STANLEY, in press). Distinguishing features are dispersed macro- and microfauna in dark muds (unit F), followed upsection by thick layers of concentrated shells (unit G). Both units display some dispersed calcareous nodules, and there is an absence of gypsum. The fauna is of a type commonly found in marine seaweed communities and on hard substrates covered by soft sediment (M.P. BERNASCONI, 1992, *written communication*). Organisms in this sequence are not, however, evidence for marine conditions, but rather more permanent, shallow, inland saline lakes. These were not connected in any way with the sea: deposition occurred from ~27,000 to 19,000 and ~11,000 years BP, at times when the coastline lay as much as 50 km to the north (MALDONADO and STANLEY, 1978, 1979; SUMMERHAYES *et al.*, 1978; ABDEL WAHAB and STANLEY, 1991). A modern analog for such lagoonal-parallic shell-bearing facies in a desert setting is Birkat Karoun, the lake in the Fayoum depression south of Cairo. This salt lake, about 240 km south of the present Nile delta coast, contains species usually associated with lagoonal environments (CHEN *et al.*, 1992) or even open marine settings (PERTHUISOT *et al.*, 1990). Similar taxa, including molluscs (BERNASCONI, 1992, *written communication*), ostracods and foraminifera, were observed in sequence III. Wind-blown sandy mud (unit C) at the top of the sequence supports the hypothesis of sediment accumulating in a temporary lacustrian setting in an arid, sparsely vegetated environment.

Sequence IV is locally restricted to 5 lithosomes in the north-central region, south and southwest of Baltim. It differs petrologically from the three other stiff mud sequences in that the dark muds are much richer in plant matter. The basal deposits comprise somewhat less vegetal material (unit H) than the upper unit (I); moreover, some samples in unit I also contain minor proportions of brackish water microfossils. Both units H and I contain dispersed calcareous nodules, but no gypsum. Sequence IV, as in the case of the other 3, is commonly covered by wind-blown sandy mud. This subfacies accumulated in the north-central alluvial plain in settings with more continuous access to Nile channel flood waters. Fresh water, available for at least part of the year, sustained floral growth and preservation of plant debris. A likely environment would be marsh-like sectors adjoining seasonally flooded lakes and ponds in a semi-desert setting (*cf.* GLENNIE, 1970; MABBUTT, 1977).

COMPACT MUDS IN HOLOCENE NILE DELTA

Supplementary information on the origin of late Pleistocene stiff muds is provided by examination of Holocene fluvial sequences (~7,000 years BP to the present) of compact mud recovered in cores in the central Nile delta (Figure 1). Core S-86 was collected on the eastern levee of the Rosetta branch of the Nile, about 3 km north of Kafr El-Zaiyat. During the Holocene, before the development of the Rosetta channel, this sector was flooded by distributaries flowing toward the northwestern delta (TOUSSOUN, 1922; BELL, 1970; SAID, 1981).

Core S-87 was recovered in the delta plain between the present Damietta and Rosetta branches, 6 km SSE of the town of Tanta. This site lay to the west of, and was flooded by, the Sebennitic branch, one of the major Nile distributaries which once flowed northward across this region (TOUSSOUN, 1922; UNDP/UNESCO, 1978; SAID, 1981; SESTINI, 1989; ARBOUILLE and STANLEY, 1991; STANLEY *et al.*, 1992).

This region, about 80 km south of the modern Nile delta coast, has not been inundated by the sea during either the late Pleistocene or Holocene. However, until closure of the two dams at Aswan and development of the barrage and delta irrigation system, this sector was seasonally flooded by the Nile, usually from August to November (BUTZER, 1976; HASSAN, 1981). Mud-laden waters breached banks and overtopped natural levees that were approximately 1 to 3 m higher than the adjacent fluvial plain (*cf.* BUTZER, 1976) and deposited admixtures of clay, silt and sand. After Nile flood waters receded, the delta plain was once again subaerially exposed. During the past 7,000 years, vegetation has increasingly covered much of this low-lying surface as man intensified irrigation (BUTZER, 1976).

Compact greyish brown (5YR 3/2) mud forms most of the upper part of cores S-86 and S-87 (Figure 7F). These Holocene sections are 15.5 m and 9.0 m in length, respectively. Radiocarbon dates reveal that mud deposition in the two cores commenced ~7,000 to 6,500 years BP (Figure 14). The age of these Holocene sections and long-term averaged sediment accumulation rates (~0.15–0.59 cm/yr; Figure 14) are comparable to those of the Holocene coastal margin (silt plain, lagoon, and marsh) in the northern Nile delta (*cf.* COUTELLIER and STANLEY, 1987; ARBOUILLE and STANLEY, 1991; CHEN *et al.*, 1992; STANLEY *et al.*, 1992; WARNE and STANLEY, 1993).

Penetrometer hardness values of Holocene muds in the central delta range from 2.0 to 3.0. Thus, they are much harder than muds of equivalent age in the lower delta margin near the coast (usually 0.5 to 1.5), and almost as hard as the much older Nile alluvial plain stiff mud of late Pleistocene age (usually >3.0). Compaction of Holocene central delta muds is primarily a function of sedimentation under alternating dry and wet conditions and of long-term exposure to desiccation under arid conditions (*cf.* KOMORNIK *et al.*, 1970), rather than of sediment accumulation rate or overburden.

The greyish brown color of central delta compact muds records some oxidation, in contrast with the soft, dark olive grey muds of the delta coast marshes and lagoons which generally formed under reducing conditions. Compact Holocene muds are characterized by horizontal and sinuous laminations (Figure 6F). Root traces and small fresh water mollusc fragments are locally present. A few sections reveal mud cracks filled with sand, presumably of wind-blown origin. Holocene mud is mostly silt, with subordinate sand and clay (Table 1). The sand-size fraction is dominated by light minerals (mostly partially stained quartz of fluvial origin); heavy minerals, mica, and plant debris are accessory components. Small calcareous nodules (Figure 4D, Table 1) are characteristic. These nascent nodules are ~0.5 cm in diameter and are disseminated randomly throughout many of the Holocene stiff mud sections. The proportion of calcareous nodules in the sand-size fraction usually ranges from 20 to 30% (Table 1), but percentages tend to increase downcore. A calcareous nodule layer was noted in core S-86 (Figure 7F). The clay size fraction in the compact Holocene mud comprises about 58% smectite, 35% kaolinite and 7% illite (Table 2), values that are comparable to clay mineral composition in some late Pleistocene stiff mud samples.

Sedimentary structures, grain size, and composition of sand-size and clay fractions of the Holocene compact mud in the central Nile delta are most comparable to late Pleistocene stiff muds as described by FRIHY and STANLEY (1988), and more specifically to sequence I subfacies described in this study. Both mud deposits record flood plain deposition on a low-relief surface, under seasonally alternating wet-dry conditions in a generally warm to hot, arid climate.

Attention is also called to the absence of gypsum in Holocene compact mud sections of cores S-86 and S-87 which accumulated in the seasonally flooded central delta plain. In contrast, gypsum-bearing muds of Holocene age have formed along the northwestern delta margin (*cf.* WEST *et al.*, 1979; ALI and WEST, 1983). Both regions are affected by a seasonal wet period (rains in winter) of very short duration and arid, evaporative conditions which prevail most of the year. However, the coastal desert setting near and west of Alexandria includes prominent inland sebkha depressions in a carbonate terrain which are markedly different from the seasonally-flooded, vegetation covered central delta plain. The formation and

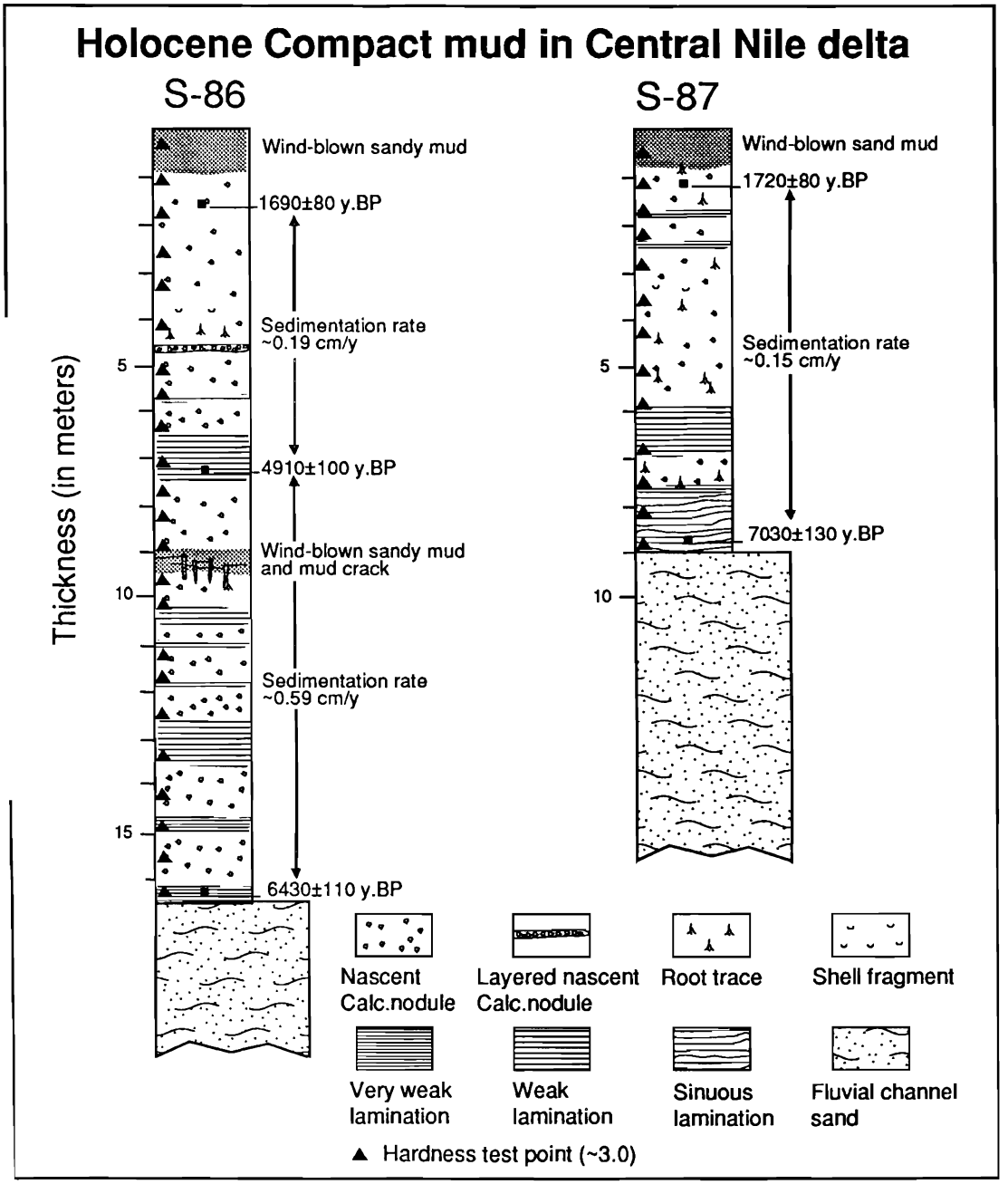

Figure 14. Lithologic logs of compact mud sections of Holocene age in two cores (S-86, S-87) recovered in the central Nile delta. Long-term averaged sedimentation accumulation rates are shown in cm/year.

preservation of gypsum in Holocene compact muds and in some late Pleistocene stiff muds (sequence II), record the coupling of quite specific depositional and climatic conditions. Gypsum-bearing stiff muds thus serve as valuable environmental markers.

PALEOGEOGRAPHY OF LATE PLEISTOCENE STIFF MUDS

Evaluation of the petrology, depositional origin and distribution of different stiff mud subfacies serves to interpret the paleogeography of the Nile alluvial plain prior to the deposition of Holocene sediment and the formation of the modern delta.

Two meandering distributaries, the Rosetta and Damietta, flow across the modern Nile delta (Figure 1), whereas during the mid-to late Holocene there were three or more meandering branches active at any one time (TOUSSOUN, 1922). The Nile system during the late Pleistocene, however, displayed a markedly different configuration.

This is deduced primarily on the basis of the nature and configuration of the stiff mud lithosomes in the north-central region: they are thicker (Figure 9D), closer together (Figure 9E), and tend to include more than 1 layer at a core locality (most are sequences I and II, Figure 9C). This configuration suggests that channels in this region were more incised. In contrast, stiff mud lithosomes are widely spaced in the northeastern and northwestern regions (Figure 9E). We suggest that mud was originally deposited in these latter sectors and was likely eroded by lateral migration and/or intensified flow.

Slope of the alluvial plain was one of the major factors controlling the above fluvial patterns. We calculate a north-dipping slope of ~0.4 to 1,000 on the late Pleistocene subaerially exposed alluvial plain. This is based on average difference in depth of stiff mud sequences and an average distance of 20 km separating profiles A-A′ near the coast and B-B′ further inland (see Figure 10). This slope was steeper than the present delta plain surface, which is only ~0.1 to 1,000 (UNDP/UNESCO, 1978). Change in slope is in part related to tectonic subsidence (*cf.* STANLEY, 1988, 1990) but, even more so, to variations in eustatic sea level. This is demonstrated by regional differences in age of the stiff mud (Figure 15A). Muds in the north-central plain began to form at about 29,000 years BP. From this time to ~18,000 years BP, sea level was substantially lowered (FAIRBANKS, 1989; PIRAZZOLI, 1992), the coastline shifted northward and the north-dipping slope of the plain increased. Lowered baseline resulted in greater entrenchment of channels in this sector.

Slope surface trends have remained relatively constant from the late Pleistocene to Holocene, *i.e.*, generally northward-directed, with some northeast and northwest components. This is indicated by orientation of the 14 elongate mud lithosomes (Figure 9E) which are primarily related to directions of former River Nile channel flow across the late Pleistocene plain. It is of note that flow patterns of seven major distributaries on the Nile delta plain remained similar to these trends during the Holocene (SAID, 1981).

Further insight on paleogeography is provided by two observations: there is an inverse relation between depth of stiff mud layers in cores and their age; and deepest sample points are not always located at core sites of youngest age (Figure 13). Analogous phenomena are noted in some modern alluvial plain profiles, where the deeper the fluvial terrace, the younger its age (Figure 13A, inset; *cf.* WALKER, 1984). We relate such regional variations in depth and age of muds to laterally migrating River Nile channels (*cf.* BUTZER, 1976:Figure 3). The averaged sample depth curve in Figure 13A indicates that terraces in the extreme northeastern and northwestern sectors are ~5 to 10 m below the present surface, respectively, and >10 to 20 m in the north-central delta. This geographic configuration favors the hypothesis proposed earlier in this section, that younger channels were located in the north-central alluvial plain (Figure 15A).

The anomalous NE–SW orientation of the mud lithosome in the Maryut lake region (Figures 9E, 15A) is primarily the result of pre-existing high-relief carbonate ridges bounding the western delta (SHUKRI *et al.*, 1956; BUTZER, 1960; WARNE and STANLEY, 1993). There is no evidence for a major channel flowing northwestwardly across this alluvial region all the way to sea: the carbonate ridges, effective barriers to flow to the former coast, diverted flow to the northeast (*i.e.* toward present Abu Qir bay). Accumulation of the thick stiff mud lithosome in the Maryut lake region is the result of fluvial sediment trapped in a large subsiding area behind (south of) the emergent ridges (WARNE and STANLEY, in press).

The absence of stiff mud in the Manzala lagoon region (Figure 15A), at least in part, may be an artifact due to higher subsidence (to 0.5 cm/yr;

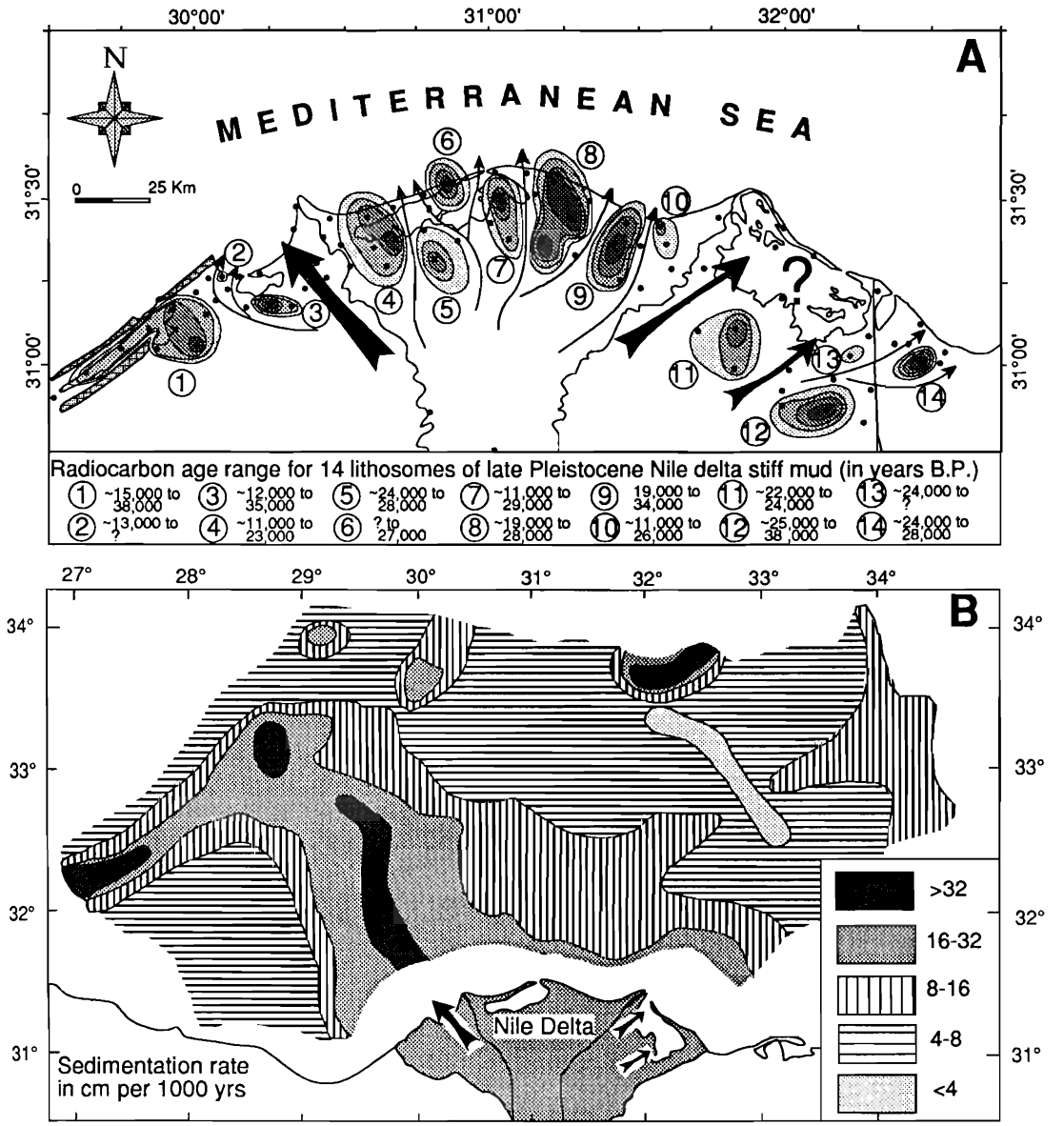

Figure 15. A, Distribution and age range of late Pleistocene stiff mud in the lower northern Nile alluvial plain: range of radiocarbon dates in the 14 lithosomes show that mud facies tend to be younger in the north-central plain. Heavy arrows indicate sectors of postulated lateral migrating channel flow and substantial fluvial erosion; light arrows show areas where channel flow was more incised. B, Map showing close relation between predominant fluvial deposition on the northwestern Nile alluvial plain (this study) and sedimentation patterns seaward on the Rosetta fan of the northwestern Nile Cone (after MALDONADO and STANLEY, 1979).

STANLEY, 1988) and greater Holocene delta plain thickness (to 50 m) in this northeastern sector. Many cores in this area have not penetrated much below uppermost late Pleistocene sections (Figure 10), and there remains the possibility that some stiff muds may actually underlie Manzala lagoon. Another explanation for the absence of stiff mud in this sector may be related to the northeast-tilt of this lowland surface (STANLEY, 1990): some mud layers were perhaps eroded by lateral migration

of former Nile channels in the sector. Erosion by channel migration may also explain the absence of mud layers in the northwest delta plain sector in the Abu Qir region (Figure 15A). A comparable situation, where fluvial erosion has removed late Pleistocene stiff mud sections, has been described in the Yangtze delta (CHEN, 1991).

Additional evidence for particularly erosive Nile flow in the northwest alluvial plain are the decreased proportions of smectite and higher relative amounts of illite in the Abu Qir sector. It is recalled that smectite grains are smaller than the other clay minerals, and have different transport, aggregation and settling attributes (SIEGEL *et al.*, 1968; STANLEY and LIYANAGE, 1986). One explanation for decreased smectite proportions may thus record preferential clay mineral size segregation and bypassing in this region as a result of intensified flow.

ALLUVIAL PLAIN STIFF MUD AS RELATED TO THE NILE SYSTEM

Integration of petrologic, stratigraphic and paleogeographic attributes serves to place lower alluvial plain mud facies in the geological context of the Nile system as a whole. Herein, we relate stiff muds underlying the northern Nile delta to some deposits of equivalent age in the Nile valley to the south, and also to sediment sections offshore on the Nile Cone to the north.

Correlation with Nile Valley

Temporal distribution of stiff muds is irregular, with prominent deposition during three phases: before 34,000 years BP, at ~28,000–22,000 years BP and ~16,000–>10,000 (Figure 12). These periods correlate rather closely with several of the more recent aggradational phases in the Nile valley (see BUTZER and HANSEN, 1968; DE HEINZELIN, 1968; HASSAN, 1976; WENDORF and SCHILD, 1976; and summary in SAID 1981:Table I-2).

Some older stiff mud layers in Smithsonian cores correspond to Korosko and Dandara aggradational phases, while the two younger periods of prominent mud accumulation (on Figure 12) correlate well with Masmas-Ballana and Sahaba-Darau aggradational phases. Higher proportions of smectite and lower of kaolinite in stiff muds also appear to correlate with these aggradational phases. Smectite is in large part derived by Blue Nile dispersal from volcanic source terrains in the Ethiopian highlands (ABU-ZEID and STANLEY, 1990).

To better interpret the origin of the alluvial stiff muds in terms of River Nile history, it is useful to note that the Sahaba-Darau aggradation had the highest floods known in the history of the Neonile (SAID, 1981). The Neonile, since Sahaba-Darau deposition, has assumed a regimen and gradient similar to those of the modern Nile. The various phases of aggradation have been related to climate change in northeastern Africa (ADAMSON *et al.*, 1980; PAULISSEN and VERMEERSCH, 1989), including the generally cooler and more humid stage from about 12,500 to 5,000 years BP (Figure 12). Thus, it is not surprising that deposition of gypsum bearing sequence II is more time-restricted (from ~34,000 to 21,000 years BP) than sequence I, and appears to have accumulated primarily during a period of increased aridity.

For detailed petrologic descriptions of various late Quaternary Nile valley deposits and their relation to climate, the reader is directed to published articles by the above-cited authors. These Nile valley formations tend to be oxidized alluvial deposits which comprise mineral suites recording primary provenance from the Ethiopian highlands (HASSAN, 1976). Independent examination of heavy minerals (FOUCAULT and STANLEY, 1989) and trace elements (HAMROUSH and STANLEY, 1990) in stiff muds of our Nile delta cores also confirms the overall importance of Blue Nile dispersal to the lower plain during the late Pleistocene.

The present investigation demonstrates that, petrologically, stiff muds in the delta borings are much more similar to late Quaternary Nile valley deposits than they are to overlying Holocene deltaic plain formations (*cf.* FRIHY and STANLEY, 1988). This is illustrated by late Pleistocene surficial stiff mud samples collected in the Nile valley south of Cairo, as described by BUTZER and HANSEN (1968), WENDORF (1986) and many others. For example, a mud-rich sample of comparable age we collected from Wadi Kubbania north of Aswan (#1; ~25,000 years BP; Table 1) has a high silt (>80%), but low sand (~10%) content. Light minerals (primarily stained quartz) predominate, and mica and calcareous nodules constitute 30% and 22%, respectively, of the sand-size fraction. Heavy minerals and gypsum are accessory components. In the clay mineral suite, smectite accounts for 51%, kaolinite 17% and illite 32%. Wadi Kubbania sample #1 is petro-

graphically most similar to calcareous nodule-bearing stiff mud subfacies in the Nile alluvial plain (Table 1).

Analysis of two other mud samples, one from Wadi Kubbania (#2, also ~25,000 years BP) and one from Beni Suef across the River Nile (>39,000 years BP), shows higher proportions of sand (~62–74%; Table 1) than in most Nile alluvial plain stiff muds. Composition of the sand size fraction, however, is quite similar: iron-stained quartz is the dominant component; carbonate nodules as well as heavy minerals, mica, gypsum, and lithic fragment are accessory constituents. Moreover, the proportion of smectite in these two samples ranges from 72 to 79%, comparable to the clay composition of the modern River Nile (Table 2). While Wadi Kubbania sample #2 and the sample from the Beni Suef region are of alluvial origin, they record a strong wind-transport influence. These two samples are in fact similar to sand-rich unit C in Nile alluvial stiff mud that are interpreted as wind-blown deposits.

Correlation with Nile Cone

Stiff muds of the Nile alluvial plain can also be correlated to late Pleistocene deposits offshore and north of the delta, on the Nile Cone. This large depocenter seaward of the Egyptian shelf is, in essence, the subaqueous depositional extension of the Nile delta (Ross and Uchupi, 1977). Late Quaternary deposits on this feature were described and their distributions mapped by Stanley and Maldonado (1977) and Maldonado and Stanley (1978, 1979). Cores collected on the Nile Cone show that, in terms of facies and accumulation rates, late Quaternary deposits younger than 58,000 years old are unevenly distributed on the Cone. The Cone sector receiving most sands and also the highest proportions of turbidite deposits during this period occurs on the Rosetta fan northwest of the Nile delta (Maldonado and Stanley, 1979:Figures 6A and 7A).

A map showing averaged long-term sedimentation accumulation rates on the Cone reveals very high rates (>32 cm/1,000 years) concentrated along a northwest linear trend extending from the Abu Qir bay region to the Rosetta fan (Figure 15B). This strongly indicates that River Nile sediments bypassed the lower delta plain and were deposited on the Cone. In the present study, evidence for this bypassing is provided by absence of stiff muds in cores in the Abu Qir-Rosetta region of the alluvial plain (Figure 15A), probably as a result of fluvial erosion. Erosion and bypassing were intensified during the last eustatic lowstand of sea level (maximum low at about 20,000–18,000 BP; *cf.* Curray, 1965; Fairbanks, 1989), when the mouth of the River Nile had migrated to the shelf edge (Maldonado and Stanley, 1979: Figure 10A).

Analysis of clay mineral distributions on the delta plain (Figure 11) and on the Nile Cone (Maldonado and Stanley, 1981) during the late Quaternary supports the above hypothesis. The average proportion of smectite in the four Nile plain stiff mud sequences (<50%) of late Pleistocene age (Table 2) is lower than that in the Nile valley (67%) mud and in compact mud of Holocene age in the central Nile delta plain (58%). Since clay minerals in all these deposits are derived essentially from a River Nile source, differences in clay mineral proportions are most likely a response to different transport process (*cf.* Stanley and Liyanage, 1986; Abu-Zeid and Stanley, 1990). Thus, the lower content of smectite in the northwestern alluvial plain (Figure 11) can be explained by intensified erosion, bypassing and seaward transport of Nile fluvial sediment from the northwestern Nile sector.

We conclude that the distribution of stiff mud deposits on the lower Nile alluvial plain can be correlated with depositional sequences in the Nile valley to the south and on the Nile Cone offshore to the north. Late Pleistocene facies throughout the region are closely related to climatic oscillations which directly influenced Nile floods, eustatic sea level stands and base level.

COMPARISON WITH ALLUVIAL MUDS IN OTHER DELTAS

As in the lower Nile delta plain, sections of stiff mud underlying Holocene deposits have been recovered in many of the world's deltas. Such mud layers were deposited on the lower alluvial plain of other deltas during the late Pleistocene at times when sea level was lower and the world's coastal plains and continental shelves were subaerially exposed.

Regardless of region, or size or nature of delta, the stiff mud units have a number of features in common. They are for the most part oxidized (usually greenish, greyish or yellow brown, and sometimes speckled), and usually show the effects of subaerial exposure. These late Pleistocene muds interfinger with iron-stained sands and, in some instances, even coarser fractions including peb-

bles. Muds commonly display horizontal lamination, and less commonly, bioturbation by benthic organisms. They not uncommonly include calcareous nodules, plant matter, burrows, root structures and, more rarely, fresh and brackish water fossils (molluscs, and in some cases, microfossils such as ostracods). The association of petrologic and biogenic features in most such deposits indicate a fluvial and/or fluviolacustrian origin.

Two late Pleistocene examples of stiff muds of approximately the same age as those underlying the Nile delta are considered for comparison: the lower Yangtze and Mississippi deltas (Figures 2 and 3). Stiff muds in these deltas are somewhat less compact (penetrometer values of ~3.0; water content from 20 to 30%) than Nile stiff muds. In the Yangtze, radiocarbon dates from cores Y-2 (ZHENG *et al.*, 1987) and Y-10 record ages of ~15,000–12,000 years BP. Stiff muds in this delta occur at depths from ~20 to 35 m. In the Mississippi, two of the stiff mud samples gave radiocarbon dates (Table 1) of ~20,000 years BP (sample WLW-18U) and ~8,000 years BP (sample 12NU-20B). The former date is closely comparable with that of lithologically equivalent late Quaternary units that are subaerially exposed (~21,000 years BP, OTVOS, 1975). Stiff muds in the lower Mississippi plain, near the present coast, are deeply buried (to depths >100 m) beneath the Recent sediment surface (KOLB and VAN LOPIK, 1966:Figure 4).

Seismic and coring surveys indicate that stiff mud units in the Mississippi delta region are thicker and laterally more continuous (FISK, 1944, 1948; U.S. CORPS OF ENGINEERS, 1958) than in the Nile (Figure 15A) and Yangtze deltas (ZHU *et al.*, 1987; ZHENG *et al.*, 1987). In both Yangtze and Mississippi deltas, the upper surfaces of mud sections are progressively shallower and locally exposed landward, and these stiff muds may interfinger with loess further inland (FISK, 1944, 1948; DANIELS and YOUNG, 1968; OTVOS, 1975; ZHENG *et al.*, 1987; CHEN, 1991; AUTIN *et al.*, 1991). Stiff muds in Yangtze delta cores can be correlated with those of the Nanhui Formation of late Pleistocene age exposed landward to the west (TANG and ZHANG, 1987). Stiff mud units underlying the Mississippi plain are attributed to the Prairie Formation (also termed Prairie Terrace or Prairie Complex; SAUCIER, 1988; AUTIN *et al.*, 1991). These late Quaternary deposits are exposed along the Gulf Coast east and west of the modern lower plain (SAUCIER and SNEAD, 1989), and are in part equivalent to the Beaumont Formation (NELSON and BRAY, 1970) to the west, in Texas, and to the Biloxi Formation (OTVOS, 1985) to the east, in western Mississippi.

Cored muds from the Yangtze delta (Figure 7G) are yellowish brown (10YR 6/6) to dark greenish grey (5G 4/1), rather than greyish brown as in the Nile delta (Figures 7A–E). Structures include poorly defined horizontal lamination. Calcareous nodules and Fe/Mn oxides are present in many core sections. Root traces are more common in the Yangtze stiff muds than in those of the Nile delta. Fresh water gastropods occur locally, including some brackish water shells in core Y-1 (for example *Arca* sp. and *Ostrea* sp.; *cf.* TANG and ZHANG, 1987). Stiff muds in cores Y-3 and Y-10 are composed of highly variable proportions of silt and clay size fractions, as in Nile delta muds (Table 1). Sand occurs in low percentages, is fine grained and composed largely of quartz. Quartz grains are less stained than in the Nile delta. Light minerals and calcareous nodules (including some calcareous aggregates) are the major sand-sized constituents (Table 1). Accessory components are heavy minerals, mica, pyrite and plant debris. The clay mineral suite is dominated by kaolinite and illite (Table 2). Late Pleistocene Yangtze delta stiff muds are most similar to calcareous nodule-bearing stiff mud (sequence I) in the Nile delta, and are similarly interpreted as flood plain deposits.

Stiff muds in the Missisippi delta (Figure 7H and I), moderate yellowish brown (10YR 5/4), are more similar in color to those in the Yangtze delta than to those in the Nile delta (Figure 7A–E). Calcareous nodules are commonly distributed in many core sections. In some cases, calcareous material occurs as filling in cracks (Figure 7I) which may have formed by decayed root tubes in swamp or marsh environments. On the basis of observation of exposures, FISK (1948) indicated that up to 50% of the stiff mud is comprised of calcareous nodules. Root traces and Fe/Mn oxide lenses also occur. Horizontal laminae, usually poorly developed, record flood events.

Mississippi delta muds, like those in the Nile and Yangtze deltas, are formed of highly variable proportions of silt and clay (Table 1). Sand is present in low proportions, and grains, for the most part, are partially stained. Major compositional components are light minerals (mostly quartz) and calcareous nodules (Table 1). Accessory components include plant debris, grains

forming Fe/Mn oxide lenses and speckled mud, and unidentified carbonate particles. Only minor amounts of heavy minerals are recorded. Shells, where present, are usually of freshwater origin; brackish water gastropods are localized in some sandy mud sections (core 12NU-20B; Table 1). The clay mineral suite comprises a somewhat larger proportion of smectite than kaolinite and illite (Table 2). Much of the late Pleistocene Mississippi delta stiff mud we examined in cores is comparable to Nile sequence I of flood plain deposition. This conforms with interpretations of exposures of equivalent age in the Mississippi valley by SAUCIER (1988), SAUCIER and SNEAD (1989) and others. Rare sections with brackish water molluscs are comparable to Nile sequence III; in the Mississippi, these deposits may record interdistributary bay and marsh environments.

Generally similar late Quaternary facies underlying Holocene sequences in other modern deltas have also been described in the literature. Examples include the Rhône (OOMKENS, 1970) and Ebro (MALDONADO, 1972) in the Mediterranean, and the Guadalupe delta of the Texas Gulf Coast (DONALDSON *et al.*, 1970). Most of these investigators recognize the alluvial origin of these muds, although some workers also allude to coastal and swamp or marsh deposition.

It is of note that the Nile, Yangtze and Mississippi deltas all lie at about the same latitude, between ~29° and 32°N (Figures 1 and 2), and each has been subject to flooding on a fairly well-defined basis. It is thus of significance that the gypsum nodule-bearing stiff mud subfacies (sequence II) found in the Nile delta is not observed in either Yangtze or Mississippi core samples. A similar subfacies, however, was examined in 1986 (field trip with Dr. R.A. Morton, Bureau of Economic Geology, Austin, Texas) in late Quaternary outcrop in the Rio Grande delta (*cf.* BROWN *et al.*, 1980). Gypsum-rich mud units are also observed in other deltas located in warm arid regions, such as the Colorado delta in the Gulf of California and the Burdekin delta on the northeastern coast of Australia. Thus, observed petrological differences (structures, various degrees of staining on quartz, presence of gypsum, faunal and floral assemblages, etc.) among stiff muds in deltas are largely attributed to marked differences in the nature of floods and sediment load, depositional environment and, in particular, climate: warm to hot and arid (Nile), warm and humid (Yangtze), and temperate (Mississippi).

Expanded study of late Quaternary core and outcrop sections in other deltas will undoubtedly reveal the presence of additional stiff mud types. Improved definition of lithofacies requires an evaluation of associated pollen, diatoms and terrigenous components in the silt fraction, and of the geochemistry of both clay and silt fractions, aspects which have remained largely neglected to date. Moreover, high-resolution subbottom profiling should complement core surveys. Paleogeographic and climatic interpretations of the type developed in this investigation are of use to archeologists working on problems of late Paleolithic settlements, of which very little is known in the Nile delta. An evaluation of the lateral continuity, thickness and physical properties of stiff mud layers underlying poorly consolidated Holocene sequences is also needed in the design and positioning of structures in deltaic regions such as the Nile. Moreover, definition of the three-dimensional configuration of stiff muds relative to interbedded sands is of direct application for hydrocarbon exploration, primarily in evaluation of the role of stiff muds as impermeable caps covering potential sand reservoirs.

SUMMARY AND CONCLUSIONS

(1) Extensive coring across the northern Nile delta reveals that the Holocene section of the lower delta plain is underlain by interfingering sand and stiff mud sequences of late Pleistocene age. The muds are compact, usually occur as a single layer in most cores, and lie at depths ranging from ~3 to 35 m below ground surface level. Fifty individual layers were recovered in 42 of 87 cores. Petrologic and stratigraphic analyses of the radiocarbon-dated (from >38,000 to ~11,000 years BP) mud serves to interpret the origin and evaluate the late Pleistocene paleogeography of the lower Nile alluvial plain.

(2) Four distinct stiff mud subfacies, or sequences, are defined on the basis of lithology, sand-size composition and clay mineralogy. Each sequence records sedimentation in a specific depositional environment. The four sequences are most reliably identified on the basis of complete stratigraphic sections, but they can also be distinguished on petrographic examination of hand specimens alone.

(3) Sequence I, a calcareous nodule-bearing stiff mud, is identified as a flood plain deposit which accumulated during two periods: >38,000–19,000

and ~14,000–11,000 years BP. Sediment, transported during floods through overflow channels and by overbank flow, was released in temporarily water-filled depressions proximal to Nile channels. Wind-blown sand accumulated on seasonally exposed playa mud surfaces. Association of petrologic features indicate that this subfacies accumulated in inland sebkhas in semi-desert, partially vegetated settings.

(4) Sequence II, a gypsum nodule-bearing stiff mud, also indicates deposition in a flood basin, but during a more restricted time frame: ~34,000–21,000 and ~13,000–12,000 years BP. Deposition prevailed in somewhat deeper, more central sectors of playas, which were more distal relative to flood channels than were sequence I sites. Wind-blown sand covers these gypsum-rich deposits, indicating that there may have been dunes in the vicinity of the playas.

(5) Sequence III, a shell-bearing stiff mud, records deposition in a shallow saline body and was even more time-restricted than sequences I and II: ~27,000–19,000 and ~11,000 years BP. The presence of organisms (molluscs, ostracods, foraminifera) typically found in lagoons and nearshore marine environments provides evidence of the more permanent nature of some shallow inland salt lakes with brackish to open marine salinities.

(6) Sequence IV, a plant debris-bearing stiff mud, indicates floral growth tolerant of freshwater to low salinity conditions; deposition prevailed from ~35,000–27,000 years BP. As in the case of sequence III, this subfacies received sufficient water for substantial plant growth and preservation, most likely in marsh-like sectors adjoining seasonally flooded playas and shallow ponds.

(7) With respect to abundance of late Pleistocene stiff mud subfacies, sequence I is the dominant subfacies: it is concentrated in 14 geographically distinct lithosomes, separated by iron-stained alluvial sand of equivalent age. Sequence II, occurs at or near the center of 9 of the 14 lithosomes; sequences III and IV are much more localized. These spatially localized areas, interpreted as playa settings, provide information as to the position and attributes of former Nile channels.

(8) Distribution of the stiff muds in time and space suggest a predominance of incised channels in the north-central plain, and more laterally migrating channels to the northeast and northwest. The Nile channel system formed earlier in the northeast and northwest sectors than in the north-central plain.

(9) Radiocarbon dating of muds shows that they were primarily deposited earlier than 34,000, and at ~28,000–22,000 and ~16,000–>10,000 years BP. The proportion of smectite, the dominant mineral in the clay assemblages, is also highest at about the same times: ~26,000–24,000, ~22,000–20,000 and ~14,000–12,000 years BP. The younger the age of a stiff mud layer, the deeper it lies below the present plain surface, indicating that deposition of muds in the lower Nile plain is related to fluvial terraces formed by migrating Nile channels.

(10) The dated muds can be correlated with several upper Pleistocene aggradational phases of the Nile mapped in upper Egypt, including the Masmas-Balana and the Sahaba-Darau. Changes with time in the proportion of clay minerals, such as smectite, in delta plain cores also correlate well with these Nile aggradational phases. The more time-restricted gypsum nodule-bearing subfacies (sequence II) appears to have accumulated primarily during a period of hyperaridity.

(11) Stiff muds on the lower Nile plain can also be correlated with deposits of equivalent age offshore, on the Nile Cone north of the present delta. Regional trends, such as absence of stiff muds and lower proportions of smectite in cores in the Abu Qir-Rosetta sector, indicate that River Nile sediments bypassed the lower northwestern delta plain and were preferentially deposited on the Rosetta fan of the northwestern Nile Cone. Channel erosion and bypassing were intensified during the last eustatic lowering and maximum lowstand of sea level, from ~27,000 to 18,000 years BP.

(12) To better interpret the origin of some late Pleistocene muds, a comparative examination was made of compact muds which accumulated in the Nile delta from middle Holocene (~7,000 years) to the present. Recent muds on the central delta plain are characterized by such features as nascent calcareous nodules and mud cracks associated with windblown sand. In this respect, central delta Holocene compact muds are comparable to late Pleistocene sequence I subfacies, *i.e.*, sediment which accumulated on a flood plain subject to alternating dry and wet conditions, and affected by dessication in a generally arid setting. Moreover, gypsum-bearing muds of Holocene age accumulating in inland sebkhas along the northwestern margin of the Nile delta may be modern

analogs for some sequence II late Pleistocene stiff muds.

(13) Nile stiff mud facies are similar in some respects to stiff mud layers of late Pleistocene age recovered in borings in other deltas. Stiff mud examined in Yangtze and Mississippi core sections, and also in some other deltas described in the literature, are most comparable to sequence I flood plain and sequence III saline lacustrian deposits. Gypsum-rich subfacies comparable to Nile sequence II are regionally more restricted to warm and hot arid regions where evaporation prevails; examples include the Rio Grande delta on the Gulf of Mexico, the Colorado delta in the Gulf of California and the Burdekin delta on the northeastern coast of Australia.

(14) Stiff muds, likely buried by Holocene sections in all major delta plains, accumulated at times of eustatic lowlands and subaerial exposure. Differences in petrology and temporal and spatial distribution patterns in the various deltas are best explained in terms of differences in depositional setting, fluvial sediment load and flood patterns, topography and especially, climate.

(15) Attributes such as lateral continuity, thickness, and physical and petrologic properties of stiff muds underlying poorly compacted deltaic plain sediments have a practical value. Applications include civil engineering and the design and construction of structures adapted to deltas. Information on the nature and configuration of stiff muds, which can serve as impermeable surfaces capping potential sand reservoirs, is also of use in hydrocarbon exploration.

ACKNOWLEDGEMENTS

Drs. A. Bassiouni, Dean, Ain Shams University, Cairo, and B. Issawi, Under Secretary for State, Cairo, are thanked for their encouragement and strong support of the Smithsonian's Nile Delta Project. This study has been made possible by the input of many Project scientists who participated directly in the collection of Nile delta cores and earlier phases of laboratory core sample analyses at the U.S. National Museum of Natural History, and particularly: Drs. D. Arbouille, V. Coutellier, H.R. Davis, H. Howa, A. Pimmel, G. Randazzo, B. Thomas, and A.G. Warne. Staff of the Department of Geography, East China Normal University, Shanghai, provided core samples and information on the Yangtze delta. Messrs. A. Blake and L.D. Britsch, U.S. Corps of Engineers, New Orleans District, generously donated valuable Mississippi delta core sections and documentation. Thanked for their assistance in the NMNH Sedimentology Laboratory are Messrs. W. Boykins and J. McRea, Jr. Dr. M.P. Bernasconi kindly identified selected molluscan assemblages. We are grateful to Drs. B.J. Willis and A.G. Warne for reviewing the manuscript. Financial support was generously provided by the Smithsonian Scholarly Studies Program, Office of the Smithsonian Assistant Secretary for Science, Office of the Director of the U.S. National Museum of Natural History, and the National Geographic Committee for Research and Exploration.

LITERATURE CITED

ABDEL WAHAB, H.S. and STANLEY, D.J., 1991. Clay mineralogy and the recent evolution of the north-central Nile delta, Egypt. *Journal of Coastal Research,* 7, 317–329.

ABU-ZEID, M.M. and STANLEY, D.J., 1990. Temporal and spatial distribution of clay minerals in Late Quaternary deposits of the Nile delta, Egypt. *Journal of Coastal Research,* 6, 677–698.

ADAMSON, D.A.; GASSE, F.; STREET, F.A., and WILLIAMS, M.A., 1980. Late Quaternary history of the Nile. *Nature,* 288, 50–55.

ALI, Y.A. and WEST, I.M., 1983. Relationships of modern gypsum nodules in sabkhas of loess to compositions of brines and sediments in northern Egypt. *Journal of Sedimentary Petrology,* 53, 1151–1168.

ARBOUILLE, D. and STANLEY, D.J., 1991. Late Quaternary evolution of the Burullus lagoon region, north-central Nile delta, Egypt. *Marine Geology,* 99, 45–66.

ATTIA, M.I., 1954. *Deposits in the Nile Valley and the Delta.* Cairo: Geological Survey of Egypt, 356p.

AUTIN, W.J.; BURNS, S.F.; MILLER, B.J.; SAUCIER, R.T., and SNEAD, J.I., 1991. Quaternary ecology of the lower Mississippi valley. *In:* MORRISON, R.B. (ed.), *Quaternary Nonglacial Geology: Conterminous U.S., The Geology of North America,* vol. K-2. The Geological Society of America, pp. 547–582.

BELL, B., 1970. The oldest records of Nile floods. *Geographical Journal,* 136, 569–573.

BROWN, L.F., JR.; BREWTON, T.J.; EVANS, T.J.; MCGOWEN, G.H.; WHITE, W.A.; GROAT, C.G., and FISHER, W.L., 1980. *Environmental Geologic Atlas of the Texas Coastal Zone.* Austin, Texas: Bureau of Economic Geology, University of Texas at Austin, 140p.

BUTZER, K.W., 1960. On the Pleistocene shore lines of Arabs' Gulf, Egypt. *Journal of Geology,* 68, 626–637.

BUTZER, K.W., 1976. *Early Hydraulic Civilization in Egypt.* Chicago, Illinois: University of Chicago Press, 134p.

BUTZER, K.W. and HANSEN, C.L., 1968. *Desert and River in Nubia.* Madison: The University of Wisconsin Press, 562p.

CHEN, Z., 1991. A preliminary discussion of subsidence in the southern Yangtze delta. *Science (Kuxiu),* 43, 58–59 (in Chinese).

CHEN, Z.; WARNE, A.G., and STANLEY, D.J., 1992. Late Quaternary evolution of the northwest Nile delta be-

tween Rosetta and Alexandria, Egypt. *Journal of Coastal Research,* 8, 527–561.

COLEMAN, J.M., 1982. *Deltas: Processes of Deposition and Models for Exploration,* 2nd edition. Boston, Massachusetts: International Human Resources Development Corporation, 124p.

COUTELLIER, V. and STANLEY, D.J., 1987. Late Quaternary stratigraphy and paleogeography of the eastern Nile delta, Egypt. *Marine Geology,* 77, 257–275.

CURRAY, J.R., 1965. Late Quaternary history, continental shelves of the United States. *In:* WRIGHT, H.E., Jr. and FREY, D.G. (eds.), *The Quaternary of the United States.* Princeton, New Jersey: Princeton University Press, pp. 723–735.

DANIELS, R.B. and YOUNG, K.K., 1968. Loess in south-central Louisiana. *Southeastern Geology,* 9, 9–19.

DONALDSON, A.C.; MARTIN, R.H., and KANES, W.H., 1970. Holocene Guadalupe delta of Texas Gulf Coast. *In:* MORGAN, J.P. (ed.), *Deltaic Sedimentation Modern and Ancient.* SEPM Special Publication 15, pp. 107–137.

EL-FAYOUMY, I.F.; EL SHAZLI, M. M., and HAMMAD, F.A., 1975. Geomorphology of the coastal area between Abu Qir and Rasheed (Northwest of the Nile Delta, E.A.R.). Cairo: *Faculty of Science, Cairo University Press,* pp. 135–147.

FAIRBANKS, R.G., 1989. A 17,000-year glacio-eustatic sea level record: Influence of glacial melting rates on the Younger Dryas event and deep-ocean circulation. *Nature,* 342, 637–642.

FISK, H.N., 1944. Geological investigation of the alluvial valley of the Lower Mississippi River. *U.S. Army Corps of Engineers, Mississippi River Commission, Vicksburg, Mississippi,* 78p.

FISK, H.N., 1948. Geological investigation of the lower Mermentau river basin and adjacent areas in coastal Louisiana. *U.S. Army Corps of Engineers, Mississippi River Commission, Vicksburg, Mississippi,* pp. 8–37.

FOUCAULT, A. and STANLEY, D.J., 1989. Late Quaternary paleoclimatic oscillations in east Africa recorded by heavy minerals in the Nile Delta. *Nature,* 339, 44–46.

FOURTAU, R., 1899. Sur les dépots Nilotiques. *Bulletin de la Société Géologique de France,* 35, 545–560.

FOURTAU, R., 1915. Contribution à l'étude des dépôts Nilotiques. *Mémoires de l'Institute Egyptien,* 8, 57–94.

FRIHY, O.E. and STANLEY, D.J., 1988. Texture and coarse fraction composition of Nile Delta deposits: Facies analysis and stratigraphic correlation. *Journal of African Earth Sciences,* 7, 237–255.

FRYE, K., 1981. *The Encyclopedia of Mineralogy.* Stroudsburg, Pennsylvania: Hutchinson Ross, IV, 794p.

GLENNIE, K.W., 1970. *Desert Sedimentary Environments.* Amsterdam: Elsevier, 222p.

GUSTAVSON, T.C., 1991. Buried vertisols in lacustrine facies of the Pliocene Fort Hancock Formation, Hueco, West Texas and Chihuahua, Mexico. *Geological Society of America Bulletin,* 103, 448–460.

HAMROUSH, H.A. and STANLEY, D.J., 1990. Paleoclimatic oscillations in East Africa interpreted by analysis of trace elements in Nile Delta Sediments. *Episodes,* 13, 264–269.

HASSAN, F.A., 1976. Heavy minerals and the evolution of the modern Nile. *Quaternary Research,* 6, 425–444.

HASSAN, F.A., 1981. Historical Nile floods and their implications for climatic change. *Science,* 212, 1142–1145.

DE HEINZELIN, J., 1968. Geological history of the Nile Valley in Nubia. *In:* WENDORF, F. (ed.), *The Prehistory of Nubia,* 1. Dallas, Texas: Southern Methodist University Press, pp. 19–55.

HOWA, H.L. and STANLEY, D.J., 1991. Plant-rich Holocene sequences in the northern Nile delta plain, Egypt: Petrology, distribution and depositional environments. *Journal of Coastal Research,* 7, 1077–1096.

KLAPPA, C.F., 1983. A process-response model for the formation of pedogenic calcretes. *In:* WILSON, R.C.L. (ed.), *Residual Deposits: Surface Related Weathering Processes and Material.* Oxford, London: Geological Society of London Special Publication 11, pp. 211–220.

KOLB, C.R. and VAN LOPIK, J.R., 1966. Depositional environments of the Mississippi River deltaic plain—southeastern Louisiana. *In:* SHIRLEY, M.L. (ed.), *Deltas in Their Geological Framework.* Houston: Houston Geological Society, pp. 17–61.

KOMORNIK, A.; ROHRLICH, V., and WISEMAN, G., 1970. Overconsolidation by desiccation of coastal late Quaternary clays in Israel. *Sedimentology,* 14, 125–140.

LIGHTY, R.G.; MACINTYRE, I.G., and STUCKENRATH, R., 1982. *Acropora palmata* reef framework: A reliable indicator of sea level in the western Atlantic for the past 10,000 years. *Coral Reefs,* 1, 125–130.

LOIZEAU, J.-L. and STANLEY, D.J., in press. Petrological-statistical approach to interpret recent and sub-recent lagoon subfacies, Idku, Nile delta of Egypt. *Marine Geology.*

MABBUTT, J.A., 1977. *Desert Landforms.* Canberra: Australia National University Press, 340p.

MALDONADO, A., 1972. El Delta del Ebro, Estudio Sedimentologico y Estragrafico. PH.D. Thesis (unpublished), University of Barcelona, 472p.

MALDONADO, A. and STANLEY, D.J., 1978. Nile Cone depositional processes and patterns in the Late Quaternary. *In:* STANLEY, D.J. and KELLING, G. (eds.), *Sedimentation in Submarine Canyons, Fans, and Trenches.* Stroudsburg, Pennsylvania: Dowden, Hutchinson and Ross, pp. 239–257.

MALDONADO, A. and STANLEY, D.J., 1979. Depositional patterns and late Quaternary evolution of two Mediterranean submarine fans: A comparison. *Marine Geology,* 31, 215–250.

MALDONADO, A. and STANLEY, D.J., 1981. Clay mineral distribution patterns as influenced by depositional processes in the southeastern Levantine Sea. *Sedimentology,* 28, 21–32.

MEDIBA (MEDITERANNEAN BASIN PROGRAM), 1992. *Nile Delta Project Data-Base Listings.* Washington, D.C.: Records, U.S. National Museum of Natural History, Smithsonian.

MÖRNER, N.A., 1971. Eustatic changes during the last 20,000 years and a method of separating the isostatic and eustatic factors in an uplifted area. *Palaeogeography, Palaeoclimatology, Palaeoecology,* 9, 153–181.

NELSON, H. and BRAY, E.E., 1970. Stratigraphy and history of the Holocene sediments in the Sabine-high

island area, Gulf of Mexico. *In:* MORGAN, J.P. (ed.), *Deltaic Sedimentation Modern and Ancient*. SEPM, Special Publication No. 15, pp. 48–77.

OOMKENS, E., 1970. Depositional sequences and sand distribution in the postglacial Rhône delta complex. *In:* MORGAN, J.P. (ed.), *Deltaic Sedimentation Modern and Ancient*. SEPM, Special Publication No. 15, pp. 198–212.

OTVOS, E.G., 1975. Southern limits of Pleistocene loess, Mississippi valley. *Southeastern Geology*, 17, 27–38.

OTVOS, E.G., 1985. Coastal evolution, Louisiana to northwest Florida. New Orleans, Louisiana: *The New Orleans Geological Society*, pp. 21–33.

PAULISSEN, E. and VERMEERSCH, P.M., 1989. Behaviour of large allogenous river systems: the example of the Saharan river Nile during late Quaternary. *Bulletin de la Société Géologique de France* 5, 73–83.

PERTHUISOT, J.-P.; GUELORGET, O.; IBRAHIM, A.W.; MARGEREL, J.-P.; MAURIN, A., and PIRON-FRENET, M., 1990. Organisation hydrochimique, biologique, et sédimentologique d'un lac intracontinental à peuplements lagunaires: la Birket Karoun (Fayoum, Egypte). *Geodinamica Acta*, 4, 73–89.

PIRAZZOLI, P.A., 1992. *World Atlas of Sea-Level Changes*. Amsterdam: Elsevier Oceanography Series, 58, 300p.

REINECK, H.E. and SINGH, I.B., 1980. *Depositional Sedimentary Environments*. Berlin: Springer-Verlag, 549p.

ROSS, D.A. and UCHUPI, E., 1977. The structure and sedimentary history of the southeastern Mediterranean Sea-Nile Cone area. *Bulletin of the American Association of Petroleum Geologists*, 61, 872–902.

SAID, R., 1981. *The Geological Evolution of the River Nile*. New York: Springer-Verlag, 151p.

SAUCIER, R.T., 1988. A new approach to Lower Mississippi Valley (LMV) Quaternary stratigraphic nomenclature. *Geological Society of America*, Denver (manuscript read at Annual Meeting), 11p.

SAUCIER, R.T. and SNEAD, J.I., 1989. Quaternary geology of the lower Mississippi Valley. *Louisiana Geological Survey*, map (one sheet), 1:1,100,000.

SCHOLLE, P.A.; BEBOUT, D.G., and MOORE, C.H., 1983. *Carbonate Depositional Environments*. AAPG Memoir, 33, 708p.

SCRUTON, P.C., 1960. Delta-building and the deltaic sequence. *In:* SHEPARD, F.P., PHLEGER, F.B. and VAN ANDEL, Tj.H. (eds.), *Recent Sediments, Northwest Gulf of Mexico*. Tulsa: AAPG, pp. 82–102.

SESTINI, G., 1989, Nile delta: A review of depositional environments and geological history. *In:* WHATELEY, M.G.K. and PICKERING, K.T. (eds.), *Deltas: Sites and Traps for Fossil Fuels*. Geological Society of London, Special Publication 41, 99–127.

SHUKRI, N.M.; PHILIP, G., and SAID, R., 1956. The geology of the Mediterranean coast between Rosetta and Bardia, Part II, Pleistocene sediments: Geomorphology and microfacies. *Bulletin de l'Institut d'Egypt*, 37, 395–427.

SIEGEL, R.; PIERCE, J.W.; URIEN, C.M., and STONE, I.C., JR., 1968. Clay mineralogy in the estuary of the Rio de la Plata, South America. *13th International Geological Congress*, 8, 51–59.

STANLEY, D.J., 1988. Subsidence in the northeastern Nile delta: Rapid rates, possible causes and consequences. *Science*, 240, 497–500.

STANLEY, D.J., 1989. Sediment transport on the coast and shelf between the Nile delta and Iraeli margin as determined by heavy minerals. *Journal of Coastal Research*, 5, 813–828.

STANLEY, D.J., 1990. Recent subsidence and northeast tilting of the Nile delta, Egypt. *Marine Geology*, 94, 147–154.

STANLEY, D.J. and CHEN, Z., 1991. Distinguishing sand facies in the Nile delta, Egypt, by stained grain and compositional component analyses. *Journal of Coastal Research*, 7, 863–877.

STANLEY, D.J. and HAMZA, F.H., 1992. Terrigenous-carbonate sediment interface (Late Quaternary) along the northwestern margin of the Nile Delta, Egypt. *Journal of Coastal Research*, 8, 153–171.

STANLEY, D.J. and LIYANAGE, A.N., 1986. Clay-mineral variations in the northeastern Nile Delta, as influenced by depositional processes. *Marine Geology*, 73, 263–283.

STANLEY, D.J. and MALDONADO, A., 1977. Nile Cone: Late Quaternary stratigraphy and sediment dispersal. *Nature*, 266, 129–135.

STANLEY, D.J.; WARNE, A.G.; DAVIS, H.R.; BERNASCONI, M., and CHEN, Z., 1992. Late Quaternary evolution of the north-central Nile delta from Manzala to Burullus Lagoons, Egypt. *National Geographic Research & Exploration*, 8, 22–51.

SUMMERHAYES, C.P.; SESTINI, G., and MISDORP, R., 1978. Nile Delta: Nature and evolution of continental shelf sediments. *Marine Geology*, 27, 43–65.

TANG, B. and ZHANG, Y., 1987. Study on Quaternary strata in the borehole Changjiang No. 1. *Bureau of Marine Geological Survey*, 3, 1–72 (in Chinese).

TOUSSOUN, O., 1922. Mémoires dur les anciennes branches du Nil. Époque Ancienne. *Mémoire de l'Institut d'Egypte*, 4, 212p.

UNDP/UNESCO. 1978. *Coastal Protection Studies. Project Findings and Recommendations*. UNDP/EGY/73/063, Paris, 483p.

U.S. CORPS OF ENGINEERS, 1958. Geology of the Mississippi River deltaic plain, southeastern Louisiana. Vicksburg, Mississippi: *Waterways Experiment Station*, 120p.

WALKER, R.G. (ed.), 1984. *Facies Models*, second edition. Geoscience Canada, 317p.

WATSON, A., 1979. Gypsum crusts in deserts. *Journal of Arid Environments*, 2, 3–20.

WARNE, D. and STANLEY, D.J., 1993. Late Quaternary evolution of the northwest Nile delta and adjacent coast in the Alexandria region, Egypt. *Journal of Coastal Research*, 9(1), 26–64.

WENDORF, F., 1986. *The Prehistory of Wadi Kubbaniya*. Dallas: Southern Methodist University Press, I–III, 863 pp.

WENDORF, F. and SCHILD, R., 1976. *Prehistory of the Nile Valley*. New York: Academic Press, pp. 307–309.

WEST, I.M.; ALY, Y.A., and HILMY, M.E., 1979. Primary gypsum nodules in a modern sebkha on the Mediterranean coast of Egypt. *Geology*, 7, 354–358.

WUNDERLICH, J. and ANDRES, W., 1991. Late Pleistocene and Holocene evolution of the western Nile delta and implications for its future development. *Franz Steiner Verlag*, 105–120.

ZHENG, X.; YAN, Q., and GOU, X., 1987. The windblown loess of the southern Changjiang delta in the late

period of the late Pleistocene. *In:* YAN, Q. and XU, S. (eds.), *Recent Yangtze Delta deposits.* East China Normal University Press, pp. 76–91 (in Chinese).

ZHU, S.; LU, Q.; CHEN, Y.; XI, J., and SHENG, Y., 1987. Characteristics of Holocene sedimentary provinces in Shanghai region. *In:* YAN, Q. and XU, S. (eds.), *Recent Yangtze Delta Deposits.* East China Normal University Press, pp. 174–184 (in Chinese).